Twist-two matrix elements at finite and infinite volume

William Detmold[1] and C.-J. David Lin[1,2]

[1]*Department of Physics, University of Washington, Box 351560, Seattle, Washington 98195, USA*
[2]*Institute for Nuclear Theory, University of Washington, Box 351550, Seattle, Washington 98195, USA*
(Received 14 January 2005; published 31 March 2005)

We present one-loop results for the forward twist-two matrix elements relevant to the unpolarized, helicity and transversity baryon structure functions, in partially-quenched ($N_f = 2$ and $N_f = 2 + 1$) heavy baryon chiral perturbation theory. The full-QCD limit can be straightforwardly obtained from these results and we also consider SU(2|2) quenched QCD. Our calculations are performed in finite volume as well as in infinite-volume. We discuss features of lattice simulations and investigate finite volume effects in detail. We find that volume effects are not negligible, typically around 5%–10% in current partially-quenched and full-QCD calculations, and are possibly larger in quenched QCD. Extensions to the off-forward matrix elements and potential difficulties that occur there are also discussed.

I. INTRODUCTION

The quark and gluon substructure of hadrons has been probed for many years in high energy scattering experiments. Much of the information that has been gleaned is encoded in the parton distribution functions (PDFs) that describe the longitudinal momentum distributions of quarks and gluons within hadrons. Cross sections for deep-inelastic scattering, for example, have been shown to factorize into short and long-distance contributions [1,2]. The short distance pieces (Wilson coefficients) are perturbatively calculable while the long range effects are expressed in terms of the PDFs. The utility of such PDFs is that they are universal; the same set of PDFs appear in deep-inelastic scattering, Drell-Yan processes and heavy vector boson production. Whilst PDFs are scale dependent, once they are known at one scale they can be calculated at higher scales via the DGLAP [3] evolution equations. A number of groups [4,5] have exploited the universality of PDFs and their known scale-dependence by performing global analyses of experimental data, thereby providing convenient parametrizations of the PDFs. Such parametrizations have proven very useful in testing perturbative QCD in high energy processes and constraining new physics, but nothing is learnt about the nonperturbative origins of the PDFs.

Whilst experiments continually increase our knowledge of PDFs, there is much that is still unknown. Recent results [6–8] have shown that $\bar{u}(x) \neq \bar{d}(x)$, however other simple qualitative questions such as whether $\Delta \bar{u}(x) = \Delta \bar{d}(x)$ or $s(x) = \bar{s}(x)$ remain unanswered. Even for the unpolarized valence quark distributions, information is scarce at large x and there is no experimental information about the transversity distributions. Consequently, any insight that can be gained directly from QCD would be very useful. Since the PDFs encode the soft, hadronic scale physics of QCD bound states, perturbative QCD is of little use. One can turn to models to suggest the qualitatively important features of PDFs (for example $\bar{u}(x) \neq \bar{d}(x)$ was predicted on

the basis of the pion cloud [9]), but to make concrete predictions with systematically improvable errors one must solve QCD nonperturbatively. Currently this means one must use lattice QCD.

In lattice QCD, one discretizes space-time and uses Monte-Carlo techniques to evaluate the functional integrals over the quark and gluons fields, necessarily making a Wick rotation to Euclidean space in the process. However, deep-inelastic scattering and related processes are dominated by distances that are lightlike, and as such are inaccessible in Euclidean space calculations. The way around this difficulty is provided by the operator product expansion (OPE) which relates matrix elements of certain local operators to Mellin moments of the various quark and gluon distributions (defined below). For quark distributions, the twist-two (twist = dimension − spin) operators that arise from the OPE of the bilocal light-cone operators in $N_f = 2$ QCD are

$$^{\rm QCD}\mathcal{O}^{(A)}_{\mu_0 \dots \mu_n} = i^n [\bar{\psi} \gamma_{\{\mu_0} \overset{\leftrightarrow}{D}_{\mu_1} \dots \overset{\leftrightarrow}{D}_{\mu_n\}} \tau_A \psi - {\rm traces}], \quad (1)$$

$$^{\rm QCD}\widetilde{\mathcal{O}}^{(A)}_{\mu_0 \dots \mu_n} = i^n [\bar{\psi} \gamma_{\{\mu_0} \gamma_5 \overset{\leftrightarrow}{D}_{\mu_1} \dots \overset{\leftrightarrow}{D}_{\mu_n\}} \tau_A \psi - {\rm traces}], \quad (2)$$

$$^{\rm QCD}\widetilde{\mathcal{O}}^{T;(A)}_{\mu_0 \dots \mu_{n+1}} = i^n [\bar{\psi} \sigma_{\mu_0 \{\mu_1} \gamma_5 \overset{\leftrightarrow}{D}_{\mu_2} \dots \overset{\leftrightarrow}{D}_{\mu_{n+1}\}} \tau_A \psi \\ - {\rm traces}], \quad (3)$$

where τ_A is an isospin matrix ($\tau_0 = \mathbf{1}$, $\tau_{1,2,3}$ are the Pauli matrices), $\{\dots\}$ indicates symmetrization of indices, the gauge covariant derivative $\overset{\leftrightarrow}{D}{}^\mu = \frac{1}{2}(\vec{D}{}^\mu - \overset{\leftarrow}{D}{}^\mu)$, and 'traces'' are subtracted in order that the operator transforms irreducibly under the Lorentz group. Additional twist-two operators can be built exclusively from gluon fields and towers of higher twist operators can also be constructed, but we shall not consider these here.

The above operators are related to the spin-averaged, longitudinally polarized, and transversely polarized quark distributions. We first define the Mellin moments of the

quark distributions $q = q^\uparrow + q^\downarrow$, $\Delta q = q^\uparrow - q^\downarrow$ and $\delta q = q^\top - q^\perp$ (where $q^{\uparrow(\downarrow)}$ corresponds to quarks with helicity aligned (antialigned) with that of a longitudinally polarized target, and $q^{\top(\perp)}$ corresponds to quarks with spin aligned (antialigned) with that of a transversely polarized target) for flavor q as

$$\langle x^n \rangle_q = \int_0^1 dx x^n [q(x) - (-1)^n \overline{q}(x)],$$

$$\langle x^n \rangle_{\Delta q} = \int_0^1 dx x^n [\Delta q(x) + (-1)^n \Delta \overline{q}(x)], \qquad (4)$$

$$\langle x^n \rangle_{\delta q} = \int_0^1 dx x^n [\delta q(x) - (-1)^n \delta \overline{q}(x)].$$

These moments are then related to the forward hadron matrix elements of the operators in Eqs. (1)–(3) through

$$\frac{1}{2}\sum_S \langle p, S | {}^{\mathrm{QCD}}\mathcal{O}^{(0,3)}_{\mu_0\cdots\mu_n} | p, S \rangle = 2 \langle x^n \rangle_{u\pm d} p_{\mu_0}\cdots p_{\mu_n},$$

$$\langle p, S | {}^{\mathrm{QCD}}\widetilde{\mathcal{O}}^{(0,3)}_{\mu_0\cdots\mu_n} | p, S \rangle = 2 \langle x^n \rangle_{\Delta u \pm \Delta d} S_{\{\mu_0} p_{\mu_1}\cdots p_{\mu_n\}},$$

$$\langle p, S | {}^{\mathrm{QCD}}\widetilde{\mathcal{O}}^{T;(0,3)}_{\mu_0\cdots\mu_{n+1}} | p, S \rangle = \frac{2}{M_H} \qquad (5)$$

$$\times \langle x^n \rangle_{\delta u \pm \delta d} S_{[\mu_0} p_{\{\mu_1]}\cdots p_{\mu_{n+1}\}},$$

where p is the momentum of the hadron, M_H is its mass and S is its spin. The plus or minus signs in Eq. (5) correspond to choosing isospin index 0 or 3, respectively. The corresponding off-forward matrix elements are similarly related to Bjorken-x moments of generalized parton distributions (GPDs) which shall be discussed briefly below (see [10] for a comprehensive review).

The hadronic matrix elements of the twist-two operators in Eq. (5) can be calculated using standard lattice techniques. Although a parametric form must be assumed in order to invert [11,12] the Mellin transforms, Eqs. (4), such calculations will then lead to information about the parton distributions directly from QCD.[1] However, all lattice calculations are necessarily performed on finite volumes and at finite lattice spacings. Additionally, with current computational resources, statistically meaningful simulations can only be performed at quark masses, m_q, considerably larger than those found in nature. These three restrictions have significant effects on calculations of twist-two matrix elements which must be taken into account if realistic predictions are to be made.

Conveniently, the low energy QCD dynamics that these matrix elements characterize can be described using effective field theory. Standard chiral perturbation theory (χPT) as formulated in the infinite-volume continuum allows systematic exploration of the quark-mass dependence of

low energy hadronic observables in the region where $m_\pi, |\vec{p}| < \Lambda_\chi$ where $\vec{p}$ is a typical momentum and $\Lambda_\chi \sim$ 1 GeV is the chiral symmetry breaking scale. Extensions to include finite volume (FV) and finite lattice spacing effects are also well developed (see Refs. [13,14] respectively for recent reviews) as are the modifications necessary to treat valence and sea quark masses independently—quenched and partially-quenched χPT (QχPT and PQχPT) [15–18]. In our study, we shall ignore the effects of the discretization of space-time[2] (whereby our results will only be strictly applicable to lattice calculations in which a continuum extrapolation has been performed) and consider continuum partially-quenched chiral perturbation theory in a finite spatial volume of dimension L^3. If the size of the box is large compared to the inverse pion mass (the lightest asymptotic state), $M_\pi L \gg 1$, the power counting of infinite volume χPT (p-counting) applies and the necessary modifications are easily made, replacing momentum integrals by sums over allowed momentum modes (see Refs. [20–32] for recent examples). On the other hand if $M_\pi L \sim 1$, one needs to treat pion zero modes (components of the pion field with zero momentum) carefully since they correspond to vacuum fluctuations of order unity. In such a regime, modified power countings are required [33–35]. In this analysis, we will restrict ourselves to the region $M_\pi L \gg 1$.

Using the low energy effective theory, it is possible to compute the quark mass and volume dependence of hadronic observables such as the matrix elements of twist-two operators. For the most part, the quark-mass dependence of the various twist-two matrix elements has been studied extensively [36–42] and lattice data have been analyzed assuming an infinite volume [36,43,44]. However, the volume dependence of these observables has been ignored (with the exception of the matrix element of the $n = 0$ helicity-dependent twist-two operator, the isovector axial coupling g_A [30,34]) in such analyses. Nonetheless, finite volume effects have been found to be important in many observables; here we investigate the effect they have on nucleon, and other octet baryon matrix elements of twist-two operators.

In Section II, we introduce aspects of heavy baryon chiral perturbation theory relevant for the analysis of twist-two matrix elements and define our notation. In Section III, we discuss the twist-two operators in QCD and their matching in the low-energy effective theory and present examples of results for the quark-mass dependence of the nucleon matrix elements using two degenerate flavors of quarks. Full results in the two flavor partially-quenched case and results including the strange quark are relegated to Appendices B and C respectively. In

---

[1] The reduced symmetry of the hyper-cubic lattice leads to lower dimensional operator mixing for twist-two operators with $n > 3$, and consequently calculations are only currently available for $n = 1, 2, 3$.

[2] The additional, Lorentz noninvariant contributions to unpolarized twist-two operators that must be included when the lattice spacing is nonzero have been considered in Ref. [19].

Appendix D, the quenched theory is discussed. In Section IV, we discuss the general form of finite volume corrections to these matrix elements and make comparisons with available data. Section IV C discusses the complications that arise when nonforward matrix elements are considered and Section V presents our conclusions.

II. HEAVY BARYON CHIRAL PERTURBATION THEORY

Heavy baryon chiral perturbation theory (HBχPT) was first constructed in Refs. [45–48]. In current lattice calculations, valence and sea quarks are often treated differently, with sea quarks either absent (quenched QCD) or having different masses than the valence quarks (partially-quenched QCD).[3] The extensions of HBχPT to quenched HBχPT [49] and partially-quenched HBχPT [41,42] to accommodate these modifications are also well established and have been used to calculate many baryon properties [40–42,49–53]. In this and the next sections, we will primarily focus on the two flavor partially-quenched theory; here we briefly introduce the relevant details following the conventions set out in Ref. [41]. We leave the three flavor and quenched cases to Appendices C and D.

A. Pseudo-Goldstone mesons

We consider a partially-quenched theory of valence (u, d), sea (j, l) and ghost ($\tilde{u}$, $\tilde{d}$) quarks with masses corresponding to the matrix

$$m_Q = \text{diag}(m_u, m_d, m_j, m_l, m_{\tilde{u}}, m_{\tilde{d}}), \tag{6}$$

where $m_{\tilde{u},\tilde{d}} = m_{u,d}$ such that the QCD path-integral determinants corresponding to the valence and ghost sectors exactly cancel.

The corresponding low-energy meson dynamics are described by the SU(4|2) PQχPT Lagrangian. At leading-order

$$\mathcal{L}_\Phi = \frac{f^2}{8}\text{str}[\partial^\mu\Sigma^\dagger\partial_\mu\Sigma] + \lambda\frac{f^2}{4}\text{str}[m_Q\Sigma^\dagger + m_Q\Sigma]$$
$$+ \alpha_\Phi\partial^\mu\Phi_0\partial_\mu\Phi_0 - m_0^2\Phi_0^2, \tag{7}$$

where the pseudo-Goldstone mesons are embedded non-linearly in

$$\Sigma = \xi^2 = \exp\left(\frac{2i\Phi}{f}\right), \tag{8}$$

with the matrix Φ given by

$$\Phi = \begin{pmatrix} M & \chi^\dagger \\ \chi & \tilde{M} \end{pmatrix}, \tag{9}$$

where

$$M = \begin{pmatrix} \eta_u & \pi^+ & J^0 & L^+ \\ \pi^- & \eta_d & J^- & L^0 \\ \bar{J}^0 & J^+ & \eta_j & Y_{jl}^+ \\ L^- & \bar{L}^0 & Y_{jl}^- & \eta_l \end{pmatrix}, \qquad \tilde{M} = \begin{pmatrix} \tilde{\eta}_u & \tilde{\pi}^+ \\ \tilde{\pi}^- & \tilde{\eta}_d \end{pmatrix},$$

$$\chi = \begin{pmatrix} \chi_{\eta_u} & \chi_{\pi^+} & \chi_{J^0} & \chi_{L^+} \\ \chi_{\pi^-} & \chi_{\eta_d} & \chi_{J^-} & \chi_{L^0} \end{pmatrix}. \tag{10}$$

The upper left 2×2 block of M corresponds to the usual valence-valence mesons, the lower right to sea-sea mesons and the remaining entries of M to valence-sea mesons. Mesons in $\tilde{M}$ are composed of ghost quarks and antiquarks and those in χ of ghost-valence or ghost-sea quark-antiquark pairs. Because of the graded symmetry of the partially-quenched theory, the mesons in χ are fermionic. In terms of the quark masses, the tree-level meson masses are given by

$$M^2_{\Phi_{ij}} = M^2_{\mathcal{Q}_i\mathcal{Q}_j} = \lambda[(m_Q)_{ii} + (m_Q)_{jj}], \tag{11}$$

where $\mathcal{Q} = (u, d, j, l, \tilde{u}, \tilde{d})$.

The singlet field $\Phi_0 = \text{str}(\Phi)/\sqrt{2}$ has mass m_0 at tree level. The terms proportional to α_Φ and m_0 in Eq. (7) are only relevant in the quenched theory (see Appendix D); in PQχPT and χPT the singlet mesons acquire large masses and can be integrated out. Furthermore, α_Φ is suppressed by $1/N_c$ and we set it to zero throughout.

B. Baryons

In SU(4|2) HBχPT, the physical nucleons (those composed of three valence quarks) enter as part of a **70**-dimensional representation. This is described by a three index flavor-tensor, $\mathcal{B}$ [41,42,49]. The embedding of the physical nucleon fields into $\mathcal{B}$ and the symmetry properties of $\mathcal{B}$ are described in Ref. [41]. The Δ-isobar must also be included in the theory since the mass-splitting, Δ, between the nucleon and Δ-isobar is $\sim$300 MeV, comparable to the physical pion mass (and less than pion masses used in current lattice simulations). The parameter Δ is assumed to be small compared to the chiral symmetry breaking scale. These fields are represented in a three index flavor-tensor $\mathcal{T}^\mu$ (a Rarita-Schwinger field) transforming in the **44**-dimensional representation of SU(4|2).

The relevant part of leading-order Lagrangian describing these baryons and their interactions with Goldstone mesons is

---

[3]At finite lattice spacing, different actions can even be used for the different quark sectors (e.g., staggered-sea quarks and domain-wall (DW) valence quarks), but we do not consider this complication here.

$$\mathcal{L}_B = i(\overline{\mathcal{B}}v \cdot \mathcal{D}\mathcal{B}) - i(\overline{\mathcal{T}}^{\mu}v \cdot \mathcal{D}\mathcal{T}_{\mu}) + \Delta(\overline{\mathcal{T}}^{\mu}\mathcal{T}_{\mu})$$
$$+ 2\alpha(\overline{\mathcal{B}}S^{\mu}\mathcal{B}A_{\mu}) + 2\beta(\overline{\mathcal{B}}S^{\mu}A_{\mu}\mathcal{B})$$
$$+ 2\mathcal{H}(\overline{\mathcal{T}}^{\nu}S^{\mu}A_{\mu}\mathcal{T}_{\nu}) + \sqrt{\frac{3}{2}}C[(\overline{\mathcal{T}}^{\nu}A_{\nu}\mathcal{B})$$
$$+ (\overline{\mathcal{B}}A_{\nu}\mathcal{T}^{\nu})], \tag{12}$$

where v^{μ} is the baryon velocity, S^{μ} is the covariant spin-vector [45,47] and $\mathcal{D}^{\mu}$ is the usual covariant derivative

$$\mathcal{D}^{\mu}\mathcal{B} = \partial^{\mu}\mathcal{B} + [V^{\mu}, \mathcal{B}],$$
$$\mathcal{D}^{\nu}\mathcal{T}_{\mu} = \partial^{\nu}\mathcal{T}_{\mu} + [V^{\nu}, \mathcal{T}_{\mu}]. \tag{13}$$

The vector and axial-vector currents appearing in the above expressions are given by

$$V^{\mu} = \frac{1}{2}(\xi\partial^{\mu}\xi^{\dagger} + \xi^{\dagger}\partial^{\mu}\xi),$$
$$A^{\mu} = \frac{i}{2}(\xi\partial^{\mu}\xi^{\dagger} - \xi^{\dagger}\partial^{\mu}\xi), \tag{14}$$

where ξ is defined in Eq. (8). The various Lorentz and flavor contractions (indicated by the parentheses) are defined in Ref. [41]. In order that $\mathcal{T}^{\mu}$ correctly describes the spin-3/2 sector, $v \cdot \mathcal{T} = S \cdot \mathcal{T} = 0$.

In what follows, we will substitute $\alpha = \frac{4}{3}g_A + \frac{1}{3}g_1$, $\beta = \frac{2}{3}g_1 - \frac{1}{3}g_A$, $C = -g_{\Delta N}$ and $\mathcal{H} = g_{\Delta\Delta}$ since these correspond to the usual χPT couplings when the QCD limit, where $m_j = m_u$ and $m_l = m_d$, of the theory is taken.

III. TWIST-TWO OPERATORS AND MATRIX ELEMENTS

A. Twist-two operators in $(PQ)\chi PT$

In the low energy effective theory, the twist-two quark bilinear operators in Eqs. (1)–(3) match onto hadronic analogues constructed to obey the same symmetry transformation properties. In two flavor QCD, the unpolarized and helicity operators transform as either $(\mathbf{3}, \mathbf{1}) \oplus (\mathbf{1}, \mathbf{3})$ (isovector) or $(\mathbf{1}, \mathbf{1})$ (isoscalar) of $SU(2)_L \times SU(2)_R$.

When one considers $SU(4|2)_L \times SU(4|2)_R$ partially-quenched QCD, there is more than one way to extend these operators [41,42,54]. Imposing supertracelessness and the correct QCD limit in the valence sector, the most general extension of τ_3 (isovector) to the adjoint representation of $SU(4|2)_{L,R}$ is

$$\bar{\tau}_3 = \text{diag}(1, -1, q_j, q_l, q_k, q_j + q_l - q_k). \tag{15}$$

The freedom in choosing the values of the q_i's can be advantageous in lattice simulations; certain choices of the q_i's eliminate disconnected contributions (diagrams in which the operator is on a quark line connected to the external states only through gluons which are notoriously hard to compute [55]) even away from the isospin limit. The nonuniqueness of the extension of Gell-Mann flavor matrices to PQQCD has additional consequences in that are discussed in Appendix C.

For the isosinglet operator, the most convenient choice is

$$\bar{\tau}_0 = \text{diag}(1, 1, 1, 1, 1, 1), \tag{16}$$

because it is purely in the singlet representation of $SU(4|2)$. Any other choice, such as $\text{diag}(1, 1, 0, 0, 1, 1)$ [which one might choose as disconnected diagrams would be absent], will contain contributions from other representations, and hence introduce additional low energy constants.

The transversity operators in QCD are chiral-odd and belong to the representation $(\overline{\mathbf{2}}, \mathbf{2}) \oplus (\mathbf{2}, \overline{\mathbf{2}})$. The most general choice for their extension to $SU(4|2)$ PQQCD is

$$\bar{\tau}_T = \text{diag}(1, y_i, y_j, y_k, y_l, y_m). \tag{17}$$

For this operator disconnected contributions vanish as the matrix element involves helicity flip. Thus clean calculations of $\langle x^n \rangle_{\delta u}$ and $\langle x^n \rangle_{\delta d}$ are possible.

Based on these symmetry properties, at leading-order in PQχPT the hadronic operators that match onto those of PQQCD are

$$\mathcal{O}_{\mu_0\cdots\mu_n}^{(A)} \equiv a_n^{(r_A)} \frac{i^{n+1}}{\Lambda_{\chi}^n} \frac{f^2}{4} \text{str}[\Sigma^{\dagger}\overline{\tau}_A \overrightarrow{\partial}_{\mu_0} \ldots \overrightarrow{\partial}_{\mu_n} \Sigma + \Sigma\overline{\tau}_A \overrightarrow{\partial}_{\mu_0} \ldots \overrightarrow{\partial}_{\mu_n} \Sigma^{\dagger}] + \alpha_n^{(r_A)} v_{\mu_0\cdots} v_{\mu_n}(\overline{\mathcal{B}}\mathcal{B}\overline{\tau}_A^{\xi^+})$$
$$+ \beta_n^{(r_A)} v_{\mu_0} \ldots v_{\mu_n}(\overline{\mathcal{B}}\overline{\tau}_A^{\xi^+} \mathcal{B}) + \gamma_n^{(r_A)} v_{\mu_0} \ldots v_{\mu_n}(\overline{\mathcal{T}}^{\rho}\overline{\tau}_A^{\xi^+} \mathcal{T}_{\rho}) + \sigma_n^{(r_A)} v_{\{\mu_0} \ldots v_{\mu_{n-2}}(\overline{\mathcal{T}}_{\mu_{n-1}}\overline{\tau}_A^{\xi^+} \mathcal{T}_{\mu_n\}}) - \text{traces}, \tag{18}$$

$$\widetilde{\mathcal{O}}_{\mu_0\cdots\mu_n}^{A} \equiv \Delta\alpha_n^{(r_A)} v_{\{\mu_0} \ldots v_{\mu_{n-1}}(\overline{\mathcal{B}}S_{\mu_n\}}\mathcal{B}\overline{\tau}_A^{\xi^+}) + \Delta\beta_n^{(r_A)} v_{\{\mu_0} \ldots v_{\mu_{n-1}}(\overline{\mathcal{B}}S_{\mu_n\}}\overline{\tau}_A^{\xi^+} \mathcal{B})$$
$$+ \Delta\gamma_n^{(r_A)} v_{\{\mu_0} \ldots v_{\mu_{n-1}}(\overline{\mathcal{T}}^{\rho}S_{\mu_n\}}\overline{\tau}_A^{\xi^+} \mathcal{T}_{\rho}) + \Delta\sigma_n^{(r_A)} v_{\{\mu_0} \ldots v_{\mu_{n-3}}(\overline{\mathcal{T}}_{\mu_{n-2}}S_{\mu_{n-1}}\overline{\tau}_A^{\xi^+} \mathcal{T}_{\mu_n\}})$$
$$+ (1 - \delta_{A0})\Delta c_n^{(r_A)} v_{\{\mu_0} \ldots v_{\mu_{n-1}}[(\overline{\mathcal{T}}_{\mu_n\}}\overline{\tau}_A^{\xi^+} \mathcal{B}) + (\overline{\mathcal{B}}\overline{\tau}_A^{\xi^+} \mathcal{T}_{\mu_n\}})] - \text{traces}, \tag{19}$$

$$\tilde{\mathcal{O}}^{T}_{\mu_0\dots\mu_n\alpha} \equiv \delta\alpha_n v_{\{\mu_0}\dots v_{[\mu_n]}(\overline{\mathcal{B}}S_{\alpha]}\mathcal{B}\bar{\tau}^{\xi^+_T}) + \delta\beta_n v_{\{\mu_0}\dots v_{[\mu_n]}(\overline{\mathcal{B}}S_{\alpha]}\bar{\tau}^{\xi^+_T}\mathcal{B}) + \delta\gamma_n v_{\{\mu_0}\dots v_{[\mu_n]}(\overline{\mathcal{T}}^{\rho}S_{\alpha]}\bar{\tau}^{\xi^+_T}\mathcal{T}_\rho)$$

$$+ \delta\sigma_n v_{\{\mu_0}\dots v_{\mu_{n-2}}(\overline{\mathcal{T}}_{\mu_{n-1}}S_{[\alpha}\bar{\tau}^{\xi^+_T}\mathcal{T}_{\mu_n]\}}) + \delta c_n v_{\{\mu_0}\dots v_{[\mu_n]}[(\overline{\mathcal{T}}_{\alpha]}\bar{\tau}^{\xi^+_T}\mathcal{B}) + (\overline{\mathcal{B}}\bar{\tau}^{\xi^+_T}\mathcal{T}_{\alpha]})] - \text{traces}, \quad (20)$$

where $\bar{\tau}^{\xi^\pm}_A = \frac{1}{2}(\xi^\dagger\bar{\tau}_A\xi \pm \xi\bar{\tau}_A\xi^\dagger)$ and $\bar{\tau}^{\xi^\pm_T} = \frac{1}{2}(\xi^\dagger\bar{\tau}_T\xi^\dagger \pm \xi\bar{\tau}_T\xi)$, and the different Lorentz and flavor contractions (indicated by the parentheses) are given in Ref. [41]. The superscript on the low energy constants (LECs; $\alpha^{(r_A)}$, $\Delta\sigma^{(r_A)}$, etc.) in the unpolarized and helicity operators labels the chiral representation to which they belong; for $A = 0$, $r_0 = s$ (singlet) otherwise $r_A = a$ (adjoint). In what follows, we take A to be either 0 or 3. In QCD, the two different flavor contractions of the operators proportional to $\alpha_n^{(r_A)}$ and $\beta_n^{(r_A)}$ (and their spin-dependent analogues) are identical.

There are additional classes of operators that formally enter these expressions at the same order but do not contribute to the next-to-leading order (NLO) matrix elements, i.e., their contributions to one-loop diagrams vanish; for example,

$$v_{\{\mu_0}\dots v_{\mu_{n-2}}(\overline{\mathcal{T}}_{\mu_{n-1}}S_{\mu_n\}}\bar{\tau}^{\xi^+}_A\mathcal{B}),$$
$$\text{and} \quad v_{\{\mu_0}\dots v_{\mu_{n-1}}(\overline{\mathcal{B}}S_{\mu_n\}}\tau^{\xi^-}_A\mathcal{B}). \quad (21)$$

Such operators are omitted in Eqs. (18)–(20). Also, NLO counter terms, such as

$$(\overline{\mathcal{B}}\{\tau^{\xi^+}_A, \mathcal{M}_+\}\mathcal{B}),$$
$$\text{where} \quad \mathcal{M}_+ = \frac{1}{2}(\xi^\dagger m_Q\xi^\dagger + \xi m_Q\xi), \quad (22)$$

are neglected in this work, since we are focusing on finite volume effects arising from one-loop diagrams at NLO. For the unpolarized isovector operators, these counter

terms are explicitly displayed in Ref. [41]; for the other operators, they are simple generalizations.

Additional, higher-order operators arise when powers of the baryon velocity are replaced by derivatives, such as $v_{\{\mu_0}\dots(\frac{i}{M}\partial)_{\mu_{n-1}}(\overline{\mathcal{B}}S_{\mu_n\}}\tau^{\xi^-}_A\mathcal{B})$. In the forward limit, these operators only appear in loop diagrams, so their contributions to matrix elements start at next-to-next-to-leading order (NNLO), therefore we do not include them in this work.

B. Nucleon matrix elements

The one-loop diagrams that contribute to nucleon twist-two matrix elements at NLO are shown in Fig. 1. The first two diagrams, (a) and (b), represent the wave-function renormalization while the other diagrams are operator renormalizations. Diagrams (e) and (f) are absent for the unpolarized or isoscalar operator matrix elements as the transition between **70**-plet and **44**-plet baryon states changes spin and isospin. Finally, diagrams in which the twist-two operator is inserted on a meson line [(g), (h) and (j)] are only present in the spin-averaged cases.

In Appendices B, C, and D, we give the results for the independent matrix elements in SU(4|2) PQχPT, for SU(6|3) PQχPT and for SU(2|2) quenched χPT in the isospin limit. As an example, here we present the SU(4|2) isospin limit ($m_u = m_d$, $m_j = m_l$), $q_j = q_l$ result for the nucleon matrix element of the isovector, unpolarized operators $\mathcal{O}^{(3)}_{\mu_0\dots\mu_n}$:

$$\langle N|\mathcal{O}^{(3)}_{\mu_0\dots\mu_n}|N\rangle = \frac{1}{3}\overline{U}_p v_{\mu_0}\dots v_{\mu_n}U_p(2\alpha_n^{(a)} - \beta_n^{(a)}) \times [1 + (1 - \delta_{n0})\mathcal{W}_{SU(4|2)}]$$

$$+ \frac{i(1 - \delta_{n0})}{6f^2}v_{\mu_0}\dots v_{\mu_n}\left\{\frac{8}{3}g_{\Delta N}^2\left(\gamma_n^{(a)} - \frac{\sigma_n^{(a)}}{3}\right)[3\mathcal{H}(M_\pi, \Delta) + 2\mathcal{H}(M_{uj}, \Delta)] + \alpha_n^{(a)}[8i I(M_{uj})\right.$$

$$- 3\mathcal{H}(M_{uj}, 0)(2g_1 g_A + 3g_1^2) + 3\mathcal{H}(M_\pi, 0)(2g_A^2 + 2g_1 g_A + 3g_1^2) + 12\delta^2(g_1 + g_A)^2\mathcal{H}_{\eta'}(M_\pi, 0)]$$

$$\left. - \beta_n^{(a)}[4i I(M_{uj}) - 12\mathcal{H}(M_{uj}, 0)g_1 g_A + 3\mathcal{H}(M_\pi, 0)(4g_1 g_A + g_A^2) + 6\delta^2(g_1 + g_A)^2\mathcal{H}_{\eta'}(M_\pi, 0)]\right\},$$

$$(23)$$

where $\mathcal{W}_{SU(4|2)}$ is the nucleon wave-function renormalization given in Eq. (B1) and

$$\delta^2 = M_\pi^2 - M_{uj}^2 = \lambda(m_u - m_j), \quad (24)$$

is proportional to the difference between sea and valence quark masses. The functions $I(M)$, $\mathcal{H}(M, \Delta)$ and $\mathcal{H}_{\eta'}(M, \Delta)$ are defined in Eqs. (A1),(33) and (34), below. Finally, U_B corresponds to the type B baryon spinor. To take the QCD limit, we would set $\delta \to 0$ and $j \to u$. For equivalent choices of the $\bar{\tau}_A$ our results reproduce those

found previously for the unpolarized isovector operator [41,42]. One can also calculate the matrix elements of these operators in the Δ-isobar (and the N-Δ transition in the spin-dependent cases). However since these are not stable particles in much of the region where χPT converges, we do not present the expressions.

In these results, the only effect of the diagrams in which the twist-two operator couples to a meson (diagrams (g), (h) and (j) in Fig. 1) is to satisfy the number sum rule for the $n = 0$ matrix elements, producing the δ_{n0} factors in the
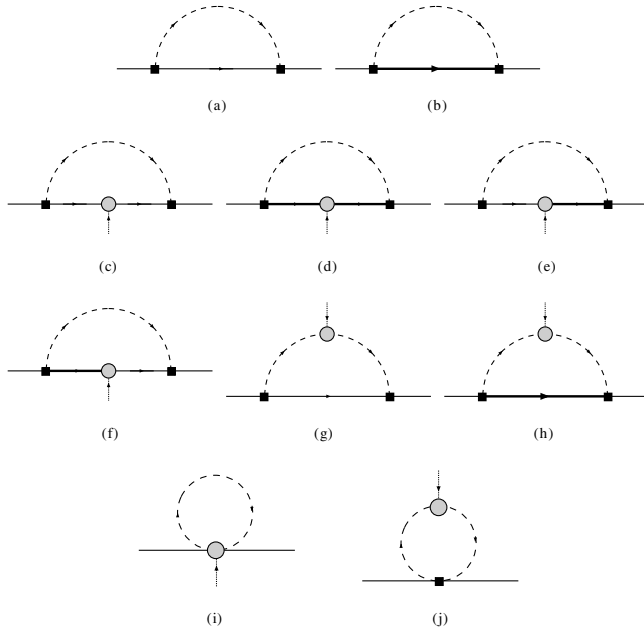
FIG. 1. Diagrams contributing to nucleon matrix elements of the twist-two operators. The black square corresponds to an interaction from the strong Lagrangian and the gray circle represents an insertion of the twist-two operators in Eqs. (18)–(20). The thin, thick and dashed lines are **70**-plet baryons, **44**-plet baryons and mesons, respectively. The first two diagrams represent the wave-function renormalization and the remainder are operator renormalizations. Diagrams (e) and (f) are absent for the unpolarized, and isoscalar operator matrix elements, and diagrams in which the twist-two operator is inserted on a meson line are only present in the unpolarized case.

above expression. For $n > 0$, these diagrams give subleading contributions, entering at $\mathcal{O}(p^{n+2})$. The number sum-rule also fixes

$$2\alpha_0^{(a)} - \beta_0^{(a)} = 3, \qquad \gamma_0^{(a)} = 3, \qquad \sigma_0^{(a)} = 0,$$
$$\alpha_0^{(s)} + \beta_0^{(s)} = 3, \qquad \gamma_0^{(s)} = 3, \qquad \sigma_0^{(s)} = 0, \tag{25}$$

and the $n = 0$ low-energy constants of the spin-dependent operators can be fixed in terms of the usual axial couplings

$$2\Delta\alpha_0^{(a)} - \Delta\beta_0^{(a)} = 6g_A, \qquad \Delta\gamma_0^{(a)} = 2g_{\Delta\Delta},$$
$$\Delta\sigma_0^{(a)} = 0, \qquad \Delta c_0^{(a)} = -\sqrt{\frac{3}{2}}g_{\Delta N},$$
$$\Delta\alpha_0^{(s)} + \Delta\beta_0^{(s)} = 2(g_A + g_1), \qquad \Delta\gamma_0^{(s)} = 0, \tag{26}$$
$$\Delta\sigma_0^{(s)} = 0.$$

IV. FINITE VOLUME CORRECTIONS

A. General discussion

In momentum space, the finite volume of a lattice simulation restricts the available momentum modes. Here we

shall consider a hyper-cubic box of dimensions $L^3 \times T$ with $T \gg L$. Imposing periodic boundary conditions on mesonic fields leads to quantized momenta $k = (k_0, \vec{k})$, $\vec{k} = 2\pi/L\vec{j} = 2\pi/L(j_1, j_2, j_3)$ with $j_i \in \mathbb{Z}$, but k_0 treated as continuous. On such a finite volume, spatial momentum integrals are replaced by sums over the available momentum modes. This leads to modifications of the infinite volume results presented in the previous section; the various functions arising from loop integrals are replaced by their FV counterparts. In a system where $M_\pi L \gg 1$, finite volume effects are predominantly from Goldstone mesons propagating to large distances where they are sensitive to boundary conditions and can even "wrap around the world". Since the lowest momentum mode of the Goldstone propagator is $\sim \exp(-M_\pi L)$ in position space, finite volume effects will behave as a polynomial in $1/L$ times this exponential if no multiparticle thresholds are reached in the loop.

To investigate this behavior, we consider the various finite volume sums occurring in the twist-two matrix elements. We first define

$$\frac{1}{L^3}\sum_{\vec{k}}\int dk_0 \frac{k_\mu k_\nu}{(k^2 - m^2 + i\epsilon)(k \cdot v - \Delta + i\epsilon)}$$
$$- \frac{ig_{\mu\nu}}{16\pi^2}\bar{\lambda}\left(\frac{2\Delta^2}{3} - m^2\right)\Delta$$
$$= g_{\mu\nu}\mathcal{F}(m, \Delta) + v_\mu v_\nu \mathcal{G}(m, \Delta), \tag{27}$$

where the ultraviolet divergence has been subtracted in dimensional regularisation[4] with $\bar{\lambda} = \frac{2}{4-d} - \gamma_E + \log(4\pi) + 1$ (d is the number of dimensions). All finite volume sums that occur in the baryon wave-function and operator renormalizations involving baryon propagators (diagrams (a)–(h) in Fig. 1, sunset-type diagrams) can be expressed in terms of $\mathcal{F}(m, \Delta)$ and its derivatives. The tadpole diagrams in Fig. 1 are discussed in Appendix A. In the baryon rest frame where $v = (1, 0, 0, 0)$, Poisson's summation formula allows us to decompose $\mathcal{F}$ into its infinite-volume limit and a volume-dependent part,

$$\mathcal{F}(m, \Delta) = F(m, \Delta) + F^{\text{FV}}(m, \Delta). \tag{28}$$

It is straightforward to show that the infinite volume piece is

---

[4]It is important to note that because of the separation of scales, FV effects (infrared) are essentially independent of method chosen to regulate the divergent integrals (ultraviolet). Also, the results presented in this work are derived in Minkowski space. We are free to work in Minkowski space since the sicknesses of quenched and partially-quenched theories discussed in Refs. [20,56] do not occur in our calculations.

$$F(m, \Delta) = \frac{i}{16\pi^2}\left\{\left[m^2 - \frac{2\Delta^2}{3}\right]\Delta \log\left(\frac{m^2}{\mu^2}\right) + \left[\frac{10\Delta^2}{9} - \frac{4m^2}{3}\right]\Delta + \frac{2}{3}(\Delta^2 - m^2)^{3/2}\log\left(\frac{\Delta - \sqrt{\Delta^2 - m^2 + i\epsilon}}{\Delta + \sqrt{\Delta^2 - m^2 + i\epsilon}}\right)\right\} \quad (29)$$

(μ is the renormalization scale), and the finite volume corrections are given by

$$F^{\mathrm{FV}}(m, \Delta) = \frac{i}{12\pi^2}\sum_{\vec{u}\neq 0}\frac{1}{uL}\int_0^\infty d|\vec{k}|\frac{|\vec{k}|\sin(u|\vec{k}|L)}{\sqrt{|\vec{k}|^2 + m^2} + \Delta}\left(\Delta + \frac{m^2}{\sqrt{|\vec{k}|^2 + m^2}}\right) \overset{mL\gg1}{\longrightarrow} \frac{im^2}{24\pi}\sum_{\vec{u}\neq 0}\frac{\mathrm{e}^{-umL}}{uL}\mathcal{A}, \quad (30)$$

where $\vec{u} = (u_1, u_2, u_3)$ with $u_i \in \mathbb{Z}$, $u \equiv |\vec{u}|$ and

$$\mathcal{A} = \mathrm{e}^{(z^2)}[1 - \mathrm{Erf}(z)] + \left(\frac{1}{umL}\right)\left[\frac{1}{\sqrt{\pi}}\left(\frac{9z}{4} - \frac{z^3}{2}\right)\right.$$
$$+ \left(\frac{z^4}{2} - 2z^2\right)\mathrm{e}^{(z^2)}(1 - \mathrm{Erf}(z))\right] - \left(\frac{1}{umL}\right)^2$$
$$\times \left[\frac{1}{\sqrt{\pi}}\left(-\frac{39z}{64} + \frac{11z^3}{32} - \frac{9z^5}{16} + \frac{z^7}{8}\right)\right.$$
$$- \left(-\frac{z^6}{2} + \frac{z^8}{8}\right)\mathrm{e}^{(z^2)}(1 - \mathrm{Erf}(z))\right] + \mathcal{O}\left(\frac{1}{(umL)^3}\right),$$

with $\quad (31)$

$$z = \left(\frac{\Delta}{m}\right)\sqrt{\frac{umL}{2}}. \quad (32)$$

Higher order terms in the $1/(umL)$ expansion in Eq. (31) are easily calculated. For convenience, we also define the functions

$$\mathcal{H}(m, \Delta) \equiv \frac{\partial\mathcal{F}(m, \Delta)}{\partial\Delta},$$
$$\mathcal{K}(m, \Delta) \equiv \frac{\mathcal{F}(m, \Delta) - \mathcal{F}(m, 0)}{\Delta}, \quad (33)$$

and their finite volume counterparts which we denote by the corresponding roman letter with the superscript FV as in Eq. (28), e.g. $\mathcal{K} \to K^{\mathrm{FV}}$.

The function $\mathcal{A}$ represents the modification of the FV effects due to the mass-splitting Δ; in the limit $\Delta \to 0$, $\mathcal{A} \to 1$. Figure 2 shows the dependence of FV effects on the scale Δ for the functions $H^{\mathrm{FV}}(m, \Delta)$ and $K^{\mathrm{FV}}(m, \Delta)$ that arise from diagrams (a)–(f) in Fig. 1. It is clear that finite volume effects in individual diagrams involving a **44**-plet are suppressed relative to those involving only meson and **70**-plet baryon propagators, though this can be compensated for by large coefficients. A very similar result was found in the heavy meson sector [23] where the contributions involving B^* mesons are suppressed compared to those involving the B meson by the mass difference $\Delta_B = m_{B^*} - m_B$. However, the origin and behavior of the mass difference in the current context is distinct. In contrast to the heavy meson case where $\Delta_B \sim 1/m_B$ arises from the breaking of heavy-quark spin symmetry and vanishes in the heavy quark limit, the mass difference Δ is generated by strong-interaction dynamics and remains finite in the chiral limit. Empirically, Δ is almost constant over the range of quark masses considered here.

When one considers quenched or partially-quenched theories rather than standard χPT, one expects somewhat larger finite volume effects because of the enhanced long-distance behavior of double-pole structures in the singlet meson propagators of these theories [20]. These double-pole contributions are given by terms proportional to the
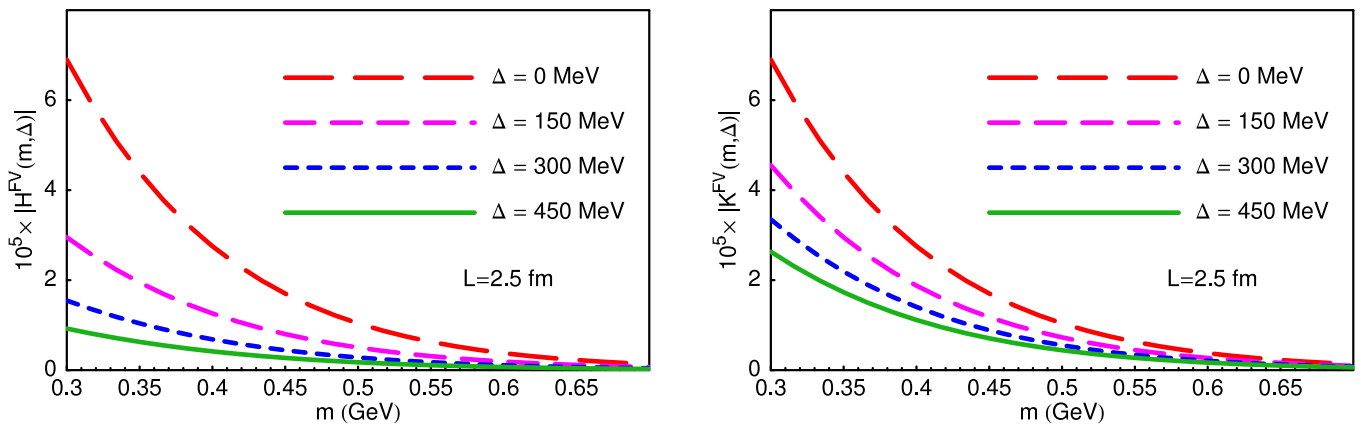

FIG. 2 (color online). Dependence of finite volume effects on the mass-splitting Δ in individual integrals/sums corresponding to diagrams (a)–(f) in Fig. 1. The point $m = 0.3$ GeV corresponds to $mL = 3.8$.

functions

$$\mathcal{H}_{\eta'}(m, \Delta) \equiv \frac{\partial \mathcal{H}(m, \Delta)}{\partial m^2},$$

$$\mathcal{K}_{\eta'}(m, \Delta) \equiv \frac{\partial \mathcal{K}(m, \Delta)}{\partial m^2}, \tag{34}$$

and the double-pole tadpole function $I_{\eta'}(m)$ given in Appendix A [and their finite volume analogues constructed as in Eq. (28)]. From Figs. 2 and 3 it is clear that $H_{\eta'}^{\mathrm{FV}}(m, \Delta)$ is about an order of magnitude larger than $H^{\mathrm{FV}}(m, \Delta)$ in accordance with expectations.

In considering the magnitude of finite volume effects, the standard chiral power counting can be misleading; the FV effects of a diagram of a given order in the power-counting may be larger than those of lower orders. For some generic observable, one may consider two contributions, C_1 and C_2, that enter at different orders, $m_1 < m_2$, in infinite volume χPT. As discussed above, the dominant finite volume effects in these contributions will typically be of the form $\delta C_i \sim (M_\pi L)^{\ell_i} \exp(-M_\pi L)$ when $M_\pi L \gg 1$ and no multiparticle on-shell intermediate states can contribute. In some situations, the presence of additional meson propagators or other infrared enhancement in the higher-order contribution (C_2) can amplify its finite volume shift relative to that of the lower-order contribution (C_1). For some (contemporarily relevant) choices of masses and volumes, the quantity

$$(M_\pi L)^{\ell_2 - \ell_1} \left(\frac{M_\pi}{\Lambda_\chi} \right)^{m_2 - m_1} > 1, \tag{35}$$

and the formally higher-order contribution will provide the dominant finite volume effect. In the current calculation, diagram (g) in Fig. 1, in which the twist-two operator is attached to mesonic propagators, may indeed fall into such a category. The finite volume corrections to these diagrams will be given by
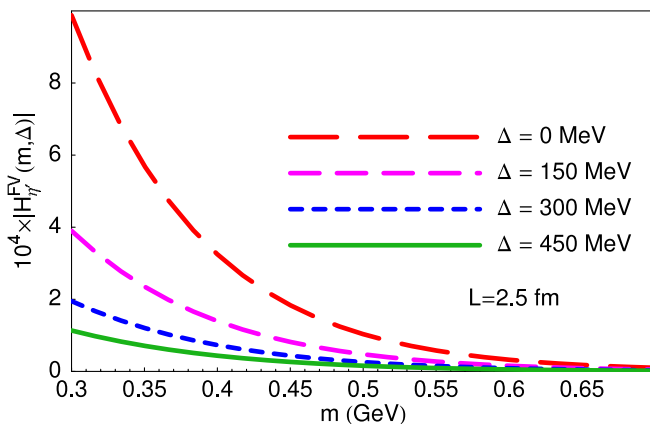

FIG. 3 (color online). Dependence of finite volume effects in double-pole contributions on the mass-splitting Δ. Note that the scale here is 10 times that in Fig. 2. The point $m = 0.3$ GeV corresponds to $mL = 3.8$.

$$\delta I_\pi^{(n)} \sim a_n^{(a)} \frac{1}{\Lambda_\chi^n} \frac{M_\pi^{n+1}}{4f^2} \frac{\partial}{\partial M_\pi^2} F^{\mathrm{FV}}(M_\pi, 0), \tag{36}$$

compared with those of the corresponding baryon operator diagrams (diagram (c) in Fig. 1)

$$\delta I_N^{(n)} \sim \frac{\alpha_n^{(a)}}{f^2} H^{\mathrm{FV}}(M_\pi, 0). \tag{37}$$

From this we see that the ratio

$$\frac{\delta I_\pi^{(n)}}{\delta I_N^{(n)}} \sim \left(\frac{M_\pi}{\Lambda_\chi} \right)^n \frac{1}{4\sqrt{M_\pi L}} \left(1 - \frac{M_\pi L}{2} \right), \tag{38}$$

where there is an undetermined coefficient involving $a_n^{(a)}$, $\alpha_n^{(a)}$ and other numerical factors that we assume to be $\mathcal{O}(1)$. Whilst formally the magnitude of this ratio is indeed greater than unity for any n in the limit $M_\pi L \to \infty$, both $\delta I_\pi^{(n)}$ and $\delta I_N^{(n)}$ are exponentially suppressed. For realistic pion masses and volumes used in current lattice simulations this ratio is consistently smaller than 1 and the FV effects of diagrams (g), (h) and (j) in Fig. 1 can be neglected. The only exception to this is in the $n = 0$ unpolarized matrix elements, the isoscalar and isovector quark numbers. Here, the volume dependence of diagrams in Fig. 1 with mesonic operators exactly cancels that of those involving baryonic operators and wave-function renormalizations to give an overall result that is independent of the volume.

B. Relevance to lattice data

Lattice calculations of twist-two matrix elements have a long history, with the first calculations occurring in the 1980s [57]. Over the last decade, a considerable effort has been made to study them in detail with major contributions from the QCDSF, LHP, RBCK and ZeRo collaborations. In Table I, recent simulation parameters are shown. State-of-the-art lattice simulations are beginning to enter the region of quark masses and lattice volumes in which the use of NLO chiral perturbation theory is justified (naively, this requires $m_\pi/\Lambda_\chi \lesssim 1/3$ and $m_\pi L \gtrsim 4$). At the moment however, there is little data in this region and a realistic fit of the combined mass and volume dependence in our PQχPT formulas (and thereby a determination of the LECs) is not possible; only general trends can be extracted.

In order to address the expected size of finite volume corrections arising from our calculation, we first define the finite volume correction

$$\langle N | \mathcal{O} | N \rangle^{\mathrm{FV}} = \frac{\langle N | \mathcal{O} | N \rangle_L^{\mathrm{one-loop}} - \langle N | \mathcal{O} | N \rangle_{L=\infty}^{\mathrm{one-loop}}}{\langle N | \mathcal{O} | N \rangle^{\mathrm{tree-level}}}, \tag{39}$$

for each of the operator matrix elements we calculate. These corrections depend on a number of low-energy constants and couplings, some of which involve the Δ resonance. In principle, all of these parameters can be extracted

TABLE I.   Summary of recent lattice calculations of nucleon twist-two matrix elements. Not all calculations involve the full set of twist-two operators.

Group	m_π [MeV]	Volume [fm^3]	Notes
Dynamical simulations ($N_f = 2$)			
QCDSF [58]	560–940	1.1^3, 1.5^3, 2.2^3	Clover, a $\sim$ 0.08–0.12 fm
LHP [59]	340	3.5^3	Staggered sea, DW valence, a $\sim$ 0.13 fm
LHP [59]	340–730	2.6^3	Staggered sea, DW valence, a $\sim$ 0.13 fm
LHP-SESAM [60]	730–900	1.6^3	Wilson, a $\sim$ 0.1 fm
LHP-SCRI [60]	480–670	1.5^3	Wilson, a $\sim$ 0.1 fm
RBCK [61]	560–700	1.9^3	DW, a $\sim$ 0.13 fm
Quenched simulations			
QCDSF [62]	580–1200	1.6^3	Clover, a $\sim$ 0.05, 0.07, 0.09 fm
QCDSF [63]	310–1000	1.5^3	Wilson, a $\sim$ 0.09 fm
QCDSF [64]	440–950	1.5^3, 2.3^3	Overlap, a $\sim$ 0.095 fm
LHP [60]	580–820	1.6^3	Wilson, a $\sim$ 0.1 fm
RBCK [65]	390–850	1.2^3, 1.6^3, 2.4^3	DW, a $\sim$ 0.15 fm
ZeRo [66]	750–910	1.1^3, 1.5^3, 2.2^3, 3.0^3	Clover, a $\sim$ 0.093 fm

from fits of the χPT forms to lattice data on nucleon matrix elements (thereby bypassing issues of the structure of unstable particles and transition matrix elements), however this is not practical at the present stage. Therefore, to fix the twist-two low-energy constants ($\alpha_n^{(a)}$, $\delta\gamma_n$ etc.) we assume that large-N_c relations [39] amongst the parton distributions in the nucleon, Δ-isobar and N–Δ transition are valid, leading to

$$\gamma_n^{(a)} = 2\alpha_n^{(a)} - \beta_n^{(a)}, \qquad \Delta\gamma_n^{(a)} = \frac{1}{5}(2\Delta\alpha_n^{(a)} - \Delta\beta_n^{(a)}),$$

$$\Delta c_n^{(a)} = \frac{1}{2}(2\Delta\alpha_n^{(a)} - \Delta\beta_n^{(a)}), \qquad \gamma_n^{(s)} = \alpha_n^{(s)} + \beta_n^{(s)}, \quad (40)$$

$$\Delta\gamma_n^{(s)} = \Delta\alpha_n^{(s)} + \Delta\beta_n^{(s)},$$

$$\delta\alpha_n = -4\delta\beta_n = \frac{4}{5}\delta\gamma_n = \frac{8}{9}\delta c_n.$$

The remaining LECs are not constrained by large-N_c relations in QCD, and for want of accurate lattice data with which to fit them, we set $\beta_n^{(a,s)} = \alpha_n^{(a,s)}$, $\Delta\beta_n^{(a,s)} = \Delta\alpha_n^{(a,s)}$ and $\sigma_n^{(a,s)} = \Delta\sigma_n^{(a,s)} = \delta\sigma_n = 0$. Throughout, we use $f = 0.132$ GeV, and keep $\Delta = 0.3$ GeV fixed independent of the quark mass. For the parameters appearing in the flavor matrices $\bar{\tau}_3$ and $\bar{\tau}_T$, we set $q_j = q_l = q_k = 0$ and $y_j = y_k = y_l = y_m = 0$, and set y_i to be either ± 1. As discussed above, if one is using lattice data to determine the LECs, the q's and y's are fixed by the details of the lattice calculation. After making all of the above substitutions, the isospin limit results become proportional to the corresponding bare matrix elements and the finite volume effects given by Eq. (39) are easily studied.

The axial couplings g_A, g_1, and $g_{\Delta N}$ occurring in our results are the chiral limit couplings and there is some uncertainty in their values. We will fix $g_A = 1.3$ (though even the chiral limit value of this is not well known [67]), $|g_{\Delta N}| = 1.5$ and vary $g_1 = \pm g_A$. In the QCD limit, results

are independent of g_1 since in this case it only involves couplings to the η' meson which remains massive in the chiral limit and can be integrated out.

Using these parameters, Figs. 4 and 5 illustrate the typical size of finite volume effects in the various matrix elements. In Fig. 4, we consider a $(2.5 \text{ fm})^3$ box with a sea quark mass set such that the corresponding sea–sea Goldstone boson has a mass $M_{jj} = 0.35$ GeV and take $g_1 = g_A$. Figure 5 is similar except here we take $g_1 = -g_A$ to show the effect of this undetermined parameter. Variation of g_A and $g_{\Delta N}$ within reasonable bounds leads to similar modifications as those for varying g_1. At the smallest pion mass in these plots, $M_\pi L \sim 3$ and one must start to worry that infinite volume p-counting is no longer appropriate; at the largest pion mass in the plots, $M_\pi/\Lambda_\chi \sim 1/2$ and one must worry that the convergence of the chiral expansion becomes questionable. From these figures, it is nevertheless apparent that NLO PQχPT predicts finite volume effects in twist-two matrix elements that are generically $\lesssim 5$–10% for the range of masses and volumes studied here. However, there is some evidence that finite volume effects from higher orders of the standard chiral power-counting can be significant [68,69].

Recently, staggered-sea, domain-wall-valence results have become available from the LHP collaboration [59] for very large volume ($L = 3.5$ fm) calculations of g_A at a pion mass of 337 MeV. Also available are results on a somewhat smaller lattice ($L = 2.6$ fm) at the same pion mass. Although these two data points are consistent within their statistical errors (which will be reduced by ongoing calculations), their central values differ by $\sim$15%. If we ignore the issues of nonlocality due to the "fourth-root" trick used in calculating the staggered quark configurations and possible unitarity violations arising from the different valence and sea quark actions (which must vanish in the $a \to 0$ limit that we have assumed), one can ask whether
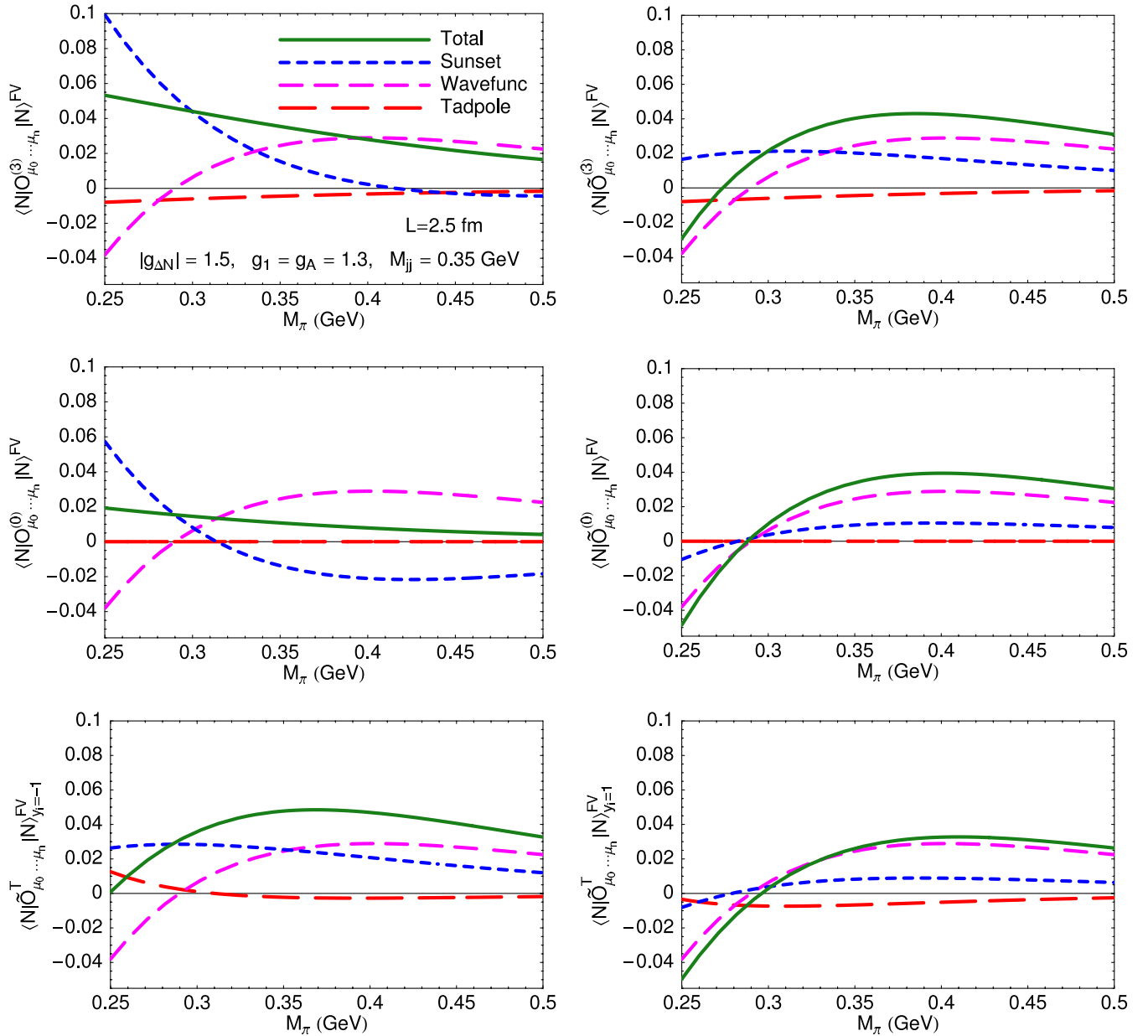
FIG. 4 (color online).   Indicative finite volume effects in SU(4|2) matrix elements. The results in the first row are for the isovector unpolarized (left) and helicity (right) operators and those in the second row are similarly for the isoscalar unpolarized (left) and helicity (right) operators. The third row corresponds to the transversity "isovector" $y_i = -1$ (left) and "isoscalar" $y_i = 1$ (right) matrix elements. In each plot, the solid curve shows the total result, while the short-, medium- and long-dashed curves correspond to the individual FV effects arising from diagrams (c)–(f), diagrams (a) and (b), and diagram (i) in Fig. 1. In all of these results, we have considered a $(2.5 \text{ fm})^3$ box and set $g_A = g_1 = 1.3$ and $|g_{\Delta N}| = 1.5$. $M_\pi = 0.25$ GeV corresponds to $M_\pi L = 3.2$.

the NLO PQχPT formulas presented here can describe this dependence. To address this question, we consider the isospin symmetric QCD limit ($m_u = m_d = m_j = m_l$) and define

$$\delta g_A = \frac{\langle N|\tilde{\mathcal{O}}_\mu^{(3)}|N\rangle_L^{\text{one-loop}} - \langle N|\tilde{\mathcal{O}}_\mu^{(3)}|N\rangle_{L=\infty}^{\text{one-loop}}}{\langle N|\tilde{\mathcal{O}}_\mu^{(3)}|N\rangle^{\text{tree-level}}}. \quad (41)$$

For this case, the LECs can be expressed in terms of the

axial couplings through Eq. (25) and the FV shift, δg_A, depends only on the pion mass, the volume and the chiral limit couplings g_A, $g_{\Delta N}$ and $g_{\Delta\Delta}$. In Fig. 6, we show the FV shift in g_A that NLO χPT predicts at the LHP pion mass, $M_\pi = 337$ MeV. To illustrate uncertainties in the results, we vary the different axial couplings. In the central fits (indicated by the curves in the plot), we set $g_A = 1.3$, $g_{\Delta N} = -1$ and $g_{\Delta\Delta} = -3$ while the shaded band corresponds to δg_A for $1.0 \leq g_A \leq 1.5$, $0 \leq |g_{\Delta N}| \leq 2$ and
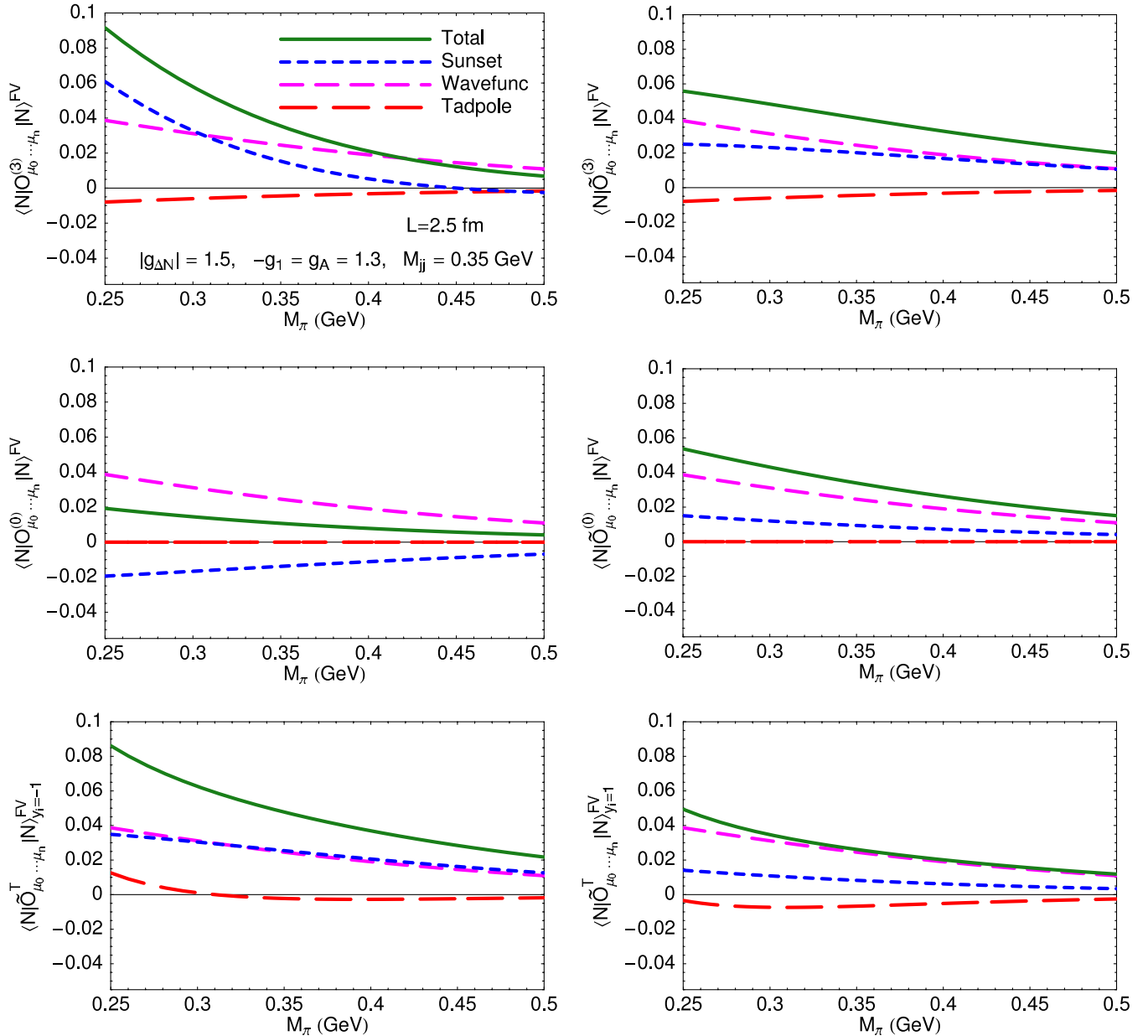
FIG. 5 (color online). As in Fig. 4 except with $g_1 = -g_A$. $M_\pi = 0.25$ GeV corresponds to $M_\pi L = 3.2$.

$g_{\Delta\Delta} = -3$. Whilst, a shift of 15% between $L = 2.6$ and 3.5 fm is not predicted, the FV effects are substantial. However, without accurate knowledge of the chiral limit couplings, even the sign of the finite volume correction to g_A is not well determined.

As discussed in the previous subsection, in quenched lattice calculations, FV effects will be enhanced because of the double-pole contributions to singlet meson propagators. In Fig. 7, we plot the volume dependence of the polarized, isovector twist-two matrix elements in SU(2|2) quenched χPT (the analytic forms of these results are presented in Appendix D). In contrast to partially-quenched χPT, in the quenched theory the LECs occurring in the Lagrangian and the twist-two operators are unrelated

to those in standard χPT (though we denote them by the same symbols for convenience). To be definite, we choose $m_0 = 0.7$ GeV and the quenched operator LECs to satisfy $\Delta\alpha_n^{(a)} = \Delta\beta_n^{(a)} = 5\Delta\gamma_n^{(a)} = 2\Delta c_n^{(a)}$ (as in the partially-quenched case), set the quenched axial couplings to $g_A = 1.3$, $|g_{\Delta N}| = 1.5$ and let g_1 and γ vary between $\pm g_A$ as indicated by the shaded region. The curves in the figure correspond to $g_1 = g_A/2$ and $\gamma = 0$. As expected, the volume dependence here is enhanced over that in the PQχPT and χPT cases.

C. Off-forward matrix elements

The off-forward matrix elements (in which the incoming and outgoing hadrons carry different momenta) of the
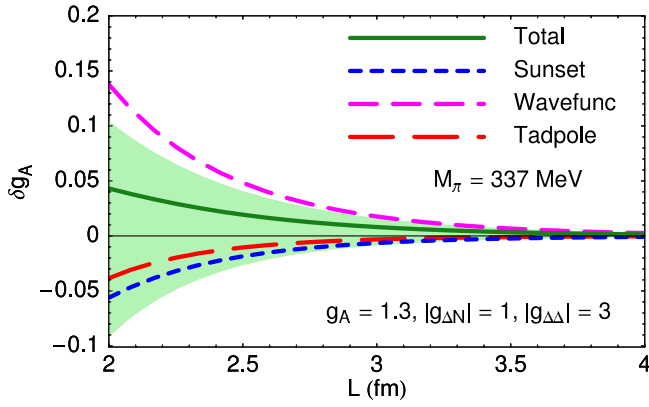
FIG. 6 (color online).   Finite volume effects in QCD calculations of g_A at $M_\pi = 337$ MeV (as appropriate for the recent LHP simulations [59]). $L = 2$ fm corresponds to $M_\pi L = 3.4$. The shaded region corresponds to varying $1.0 \leq g_A \leq 1.5$, $0 \leq |g_{\Delta N}| \leq 2$.
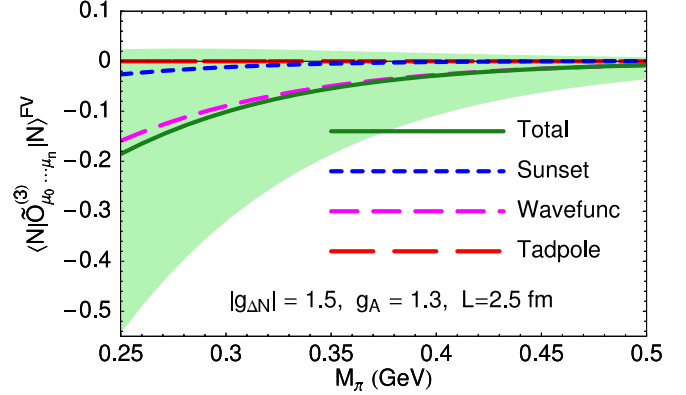
FIG. 7 (color online).   Finite volume effects in the isovector, helicity matrix elements in the proton in SU(2|2) quenched χPT. The shaded region corresponds to variation of the axial couplings g_1 and γ between $\pm g_A$ with $g_A = 1.3$, $g_{\Delta N} = 1.5$ and assuming large N_c relations for the operator LECs. The point $M_\pi = 0.25$ GeV corresponds to $M_\pi L = 3.2$.

twist-two operators correspond to moments of generalized parton distributions. Very little is known from experiment about GPDs though major programs are underway at HERMES, Jefferson Lab and COMPASS to investigate them. As such, moments of GPDs are important quantities to extract from lattice calculations and much progress is being made in this direction [70]. It is therefore important to investigate the quark mass dependence[5] and size of finite volume effects in these calculations. Here we shall only discuss the novel features that appear in regard to finite volume effects when off-forward matrix elements are considered. A full analysis of the low-energy behavior of these matrix elements will be given elsewhere [73].

To be specific, we shall consider the proton matrix elements $\langle p' | ^{\mathrm{QCD}} \mathcal{O}^{(A)}_{\mu_0 \dots \mu_n} | p \rangle$ in which four momentum $q^\mu = (p' - p)^\mu$ (with $|q^2| \ll \Lambda_\chi^2$) is injected through the twist-two operator. The analysis of these matrix elements is significantly more complicated than in the forward limit. This is primarily because the number of possible independent tensor structures in the matrix element grows with n; for example,

$$
\langle p' | ^{\mathrm{QCD}} \mathcal{O}^{(A)}_{\mu_0 \dots \mu_n} | p \rangle
$$

$$
= \overline{U}_p(p') \Bigg[\sum_{\substack{i=0 \\ \mathrm{even}}}^{n} \{ \gamma^{\{\mu_0} q^{\mu_1} \dots q^{\mu_i} \bar{p}^{\mu_{i+1}} \dots \bar{p}^{\mu_n\}} A^{(A)}_{n,i}(q^2)
$$

$$
- i \frac{q_\nu \sigma^{\nu\{\mu_0}}{2m} q^{\mu_1} \dots q^{\mu_{i-1}} \bar{p}^{\mu_i} \dots \bar{p}^{\mu_n\}} B^{(A)}_{n,i}(q^2) \}
$$

$$
+ \frac{q^{\mu_0} \dots q^{\mu_n}}{m} C^{(A)}_{n,0}(q^2) \Bigg|_{n \ \mathrm{even}} \Bigg] U_p(p), \qquad (42)
$$

---

[5]Refs. [71,72] address this issue for the infinite volume $n = 1$ matrix element relevant for the spin content of the proton in SU(2) HBχPT.

where $\bar{p} = \frac{1}{2}(p' + p)$. For each of the coefficient functions $A^{(A)}_{n,i}(q^2)$, $B^{(A)}_{n,i}(q^2)$ and $C^{(A)}_{n,0}(q^2)$, there is an independent finite volume χPT expansion.

Another complication enters when one considers the operators that match onto the twist-two operators in the low-energy effective theory. The presence of the new scale q means that considerably more operators must be included in Eqs. (18)–(20);, for example, the term proportional to $\alpha^{(r_A)}_n$ in Eq. (18) is replaced by

$$
\Bigg[\sum_{j=0}^{n} \alpha^{(r_A)}_{n,j} (v^{\{\mu_0} \dots v^{\mu_j}(-i\partial)^{\mu_{j+1}} \dots (-i\partial)^{\mu_n\}} - \mathrm{tr})
$$

$$
+ \alpha^{(r_A)}_{n,-1}((-i\partial)^{\mu_0} \dots (-i\partial)^{\mu_n} - \mathrm{tr}) \Bigg] (\overline{\mathcal{B}} \tau^A_{\xi_+} \mathcal{B}). \quad (43)
$$

Note that only terms with an even number of derivatives contribute here. Each LEC in the forward case is replaced by $\mathcal{O}(n)$ LECs. Additionally, the vector q allows more tensor structures to enter and we must also include

$$
\sum_{j=0}^{n} \hat{\alpha}^{(r_A)}_{n,j} \Bigg[v^{\{\mu_0} \dots v^{\mu_j}(-i\partial)^{\mu_{j+1}} \dots (-i\partial)^{\mu_{n-1}}
$$

$$
\times \Bigg(\overline{\mathcal{B}} \frac{[S^{\mu_n\}}, S \cdot (-i\partial)]}{M} \tau^A_{\xi_+} \mathcal{B} \Bigg) - \mathrm{tr} \Bigg], \qquad (44)
$$

since $S \cdot q \neq 0$. When we also take into account the **44**-plet fields $\mathcal{T}^\mu$, many more structures are possible since $q \cdot \mathcal{T} \neq 0$. Even for the $n < 3$ matrix elements that have been calculated on the lattice, a large number of LECs need to be determined. This makes a reliable extraction of the physical matrix elements from finite volume, unphysical mass, lattice calculations a challenging proposition.

In terms of FV effects, the modifications for the off-forward case are relatively simple and it is worthwhile to

investigate them in some detail. There are essentially two classes of diagrams: ones where the twist-two operator injects momentum into a (heavy) baryon field (e.g., (c) in Fig. 1); and ones where a meson receives the additional momentum (e.g., (h) in Fig. 1). The former class is relatively uninteresting since for heavy fields, derivatives in the twist-two operators pick out only the momentum transfer between the external states, q, and can therefore be factored out of the integral. For this type of diagram, finite volume effects will be the same as those in the forward limit as we are free to work in the Breit frame where $q \cdot v = 0$.

For diagrams in which the twist-two operator is on a meson line, the situation is different since the derivatives in the operator can result in powers of the integration momentum. The relevant integrals are of the form

$$
\frac{1}{L^3} \sum_{\vec{k}} \int \frac{dk_0}{2\pi} \frac{S \cdot (-k) S \cdot (k+q)[(-k)^{\{\mu_0} \dots (-k)^{\mu_j}(k+q)^{\mu_{j+1}} \dots (k+q)^{\mu_n\}} - \text{tr}]}{(k \cdot v - \Delta + i\epsilon)(k^2 - m^2 + i\epsilon)[(k+q)^2 - m^2 + i\epsilon]}
$$

$$
= 4 \int_0^1 dx \int_0^\infty d\lambda \frac{1}{L^3} \sum_{\vec{\ell}} \int \frac{d\ell_0}{2\pi} \frac{S \cdot (\ell+a) S \cdot (\ell+b)}{(\ell^2 - \mathcal{M}^2)^3} (-1)^j [(\ell+a)^{\{\mu_0} \dots (\ell+a)^{\mu_j}(\ell+b)^{\mu_{j+1}} \dots (\ell+b)^{\mu_n\}} - \text{tr}]
$$

$$
(45)
$$

after introducing Feynman and Schwinger parameters and shifting the momentum integration $k \to \ell = k + xq - \lambda v$. Here $a = -xq + \lambda v$, $b = (1-x)q + \lambda v$ and

$$
\mathcal{M}^2 \equiv \mathcal{M}^2(x, \lambda, m^2, q^2, \Delta)
$$
$$
= m^2 - x(1-x)q^2 + \lambda^2 + 2\lambda\Delta. \quad (46)
$$

The trace subtractions prevent any of the ℓ^{μ_i}'s arising from the operator from contracting with one another, consequently the nonvanishing scalar integrals/sums whose finite volume effects we are interested in will be of the form

$$
\int_0^1 dx \int_0^\infty d\lambda \frac{1}{L^3} \sum_{\vec{\ell}} \int \frac{d\ell_0}{2\pi} \frac{(\ell^2)^r}{(\ell^2 - \mathcal{M}^2)^3}, \quad (47)
$$

where $r = 0$, 1 or 2.

Without going into further details of the tensor structure [73], it is already clear from Eq. (46) that the effect of the momentum injection on overall finite volume shifts is very similar to the effect of the N-Δ mass-splitting. Since $x(1-x) > 0$, when spacelike momentum ($q^2 = -|\vec{q}|^2 < 0$ in Minkowski space) is injected, FV effects are suppressed as the meson receiving the momentum injection moves further away from its mass shell. However, if timelike momentum is injected the situation is more complicated. Provided the virtual particle cannot reach its mass shell, finite volume effects are enhanced over the forward case but will still remain formally exponentially suppressed. However, if the injected energy-momentum is enough to put the intermediate particles on shell, it leads to a cut in Minkowski space in infinite-volume. In this case, finite volume effects are only suppressed by powers of $1/L$ in QCD. In (partially) quenched QCD, volume corrections for isoscalar twist-two matrix elements may be proportional to positive powers of L whereby the infinite volume limit will be undefined. This suppression of finite volume effects with spacelike momentum injection and enhancement in the timelike case (which is relevant for twist-two matrix elements between states of different masses, *e.g.* $N \to \Delta$ transitions) will occur in hadronic form-factors that are specific cases of twist-two matrix elements.

V. CONCLUSIONS

We have studied the matrix elements of twist-two operators that determine the moments of the unpolarized, helicity and transversity quark distributions to NLO in (partially) quenched chiral perturbation theory in both infinite and finite volumes. We have performed our calculations in $N_f = 2$ and $N_f = 2 + 1$ partially-quenched heavy baryon chiral perturbation theory and also studied the SU(2|2) quenched theory. These results will be relevant for extrapolations of lattice calculations of these matrix elements in the proton and other octet baryons (e.g., the Λ hyperon [74]).

We have focused primarily on the effects of the finite volumes used in lattice calculations. Without accurate data in the chiral regime with which to fit the various low-energy constants on which the results depend, it is difficult to be specific, however it is clear that for most current simulations FV effects are not negligible. For typical full- or partially-quenched- QCD calculations, they are $\lesssim 5$–10% but may be significantly larger in quenched simulations.

In the case of the off-forward matrix elements relevant to generalized parton distributions, we have not presented full results for arbitrary moments [73]. However, we have analyzed the finite volume effects in these matrix elements. We find that they should decrease with respect to the forward matrix elements if spacelike momentum is injected. On the other hand if timelike momentum is transferred, finite volume effects will be enhanced; in QCD they

may become only $1/L$ suppressed, and in (partially) quenched QCD finite volume isoscalar matrix elements may even be proportional to powers of L.

ACKNOWLEDGMENTS

APPENDIX A: TADPOLE INTEGRALS AND FINITE VOLUME SUMS

The sums that appear in tadpole diagrams, after subtracting $\bar{\lambda}$, are

$$\mathcal{I}(m) = \frac{1}{L^3} \sum_{\vec{k}} \int \frac{dk_0}{2\pi} \frac{i}{k^2 - m^2 + i\epsilon} + \frac{m^2}{16\pi^2} \bar{\lambda}, \quad \text{(A1)}$$

and

$$\mathcal{I}_{\eta'}(m) = \frac{1}{L^3} \sum_{\vec{k}} \int \frac{dk_0}{2\pi} \frac{i}{(k^2 - m^2 + i\epsilon)^2} + \frac{1}{16\pi^2} \bar{\lambda}$$

$$= \frac{\partial \mathcal{I}(m)}{\partial m^2}. \quad \text{(A2)}$$

Using Poisson's summation formula, it is straightforward to show that

$$\mathcal{I}(m) = I(m) + I^{\text{FV}}(m), \quad \text{(A3)}$$

where

$$I(m) = \mu^{4-d} \int \frac{d^d k}{(2\pi)^d} \frac{i}{k^2 - m^2 + i\epsilon} + \frac{m^2}{16\pi^2} \bar{\lambda}$$

$$= \frac{m^2}{16\pi^2} \log\left(\frac{m^2}{\mu^2}\right), \quad \text{(A4)}$$

is the infinite-volume limit of $\mathcal{I}(m)$, and

$$I^{\text{FV}}(m) = \frac{m}{4\pi^2} \sum_{\vec{u} \neq \vec{0}} \frac{1}{uL} K_1(umL) \overset{mL \gg 1}{\longrightarrow} \frac{1}{4\pi^2} \sum_{\vec{u} \neq \vec{0}} \sqrt{\frac{m\pi}{2uL}}\left(\frac{1}{uL}\right)$$

$$\times e^{-umL}\left\{1 + \frac{3}{8umL} - \frac{15}{128(umL)^2}\right.$$

$$\left. + \mathcal{O}\left(\frac{1}{(umL)^3}\right)\right\}. \quad \text{(A5)}$$

APPENDIX B: RESULTS FOR SU(4|2) PQχPT

In this section, we present the results for twist-two matrix elements in the isospin limit in SU(4|2) PQχPT. The results in this and the following appendices have been independently calculated by both authors and are available on request in a *Mathematica* notebook. The various masses and the mass-splitting δ are defined in Sections II and III.

The nucleon wave-function renormalization is

$$\mathcal{W}_{SU(4|2)} = \frac{i}{2f^2}\{\mathcal{H}(M_\pi, 0)(-5g_1^2 - 4g_1 g_A + g_A^2)$$

$$+ \mathcal{H}(M_{uj}, 0)(5g_1^2 + 4g_1 g_A + 8g_A^2)$$

$$+ 4[\mathcal{H}(M_\pi, \Delta) + \mathcal{H}(M_{uj}, \Delta)]g_{\Delta N}^2$$

$$+ (-6g_1^2 - 12g_1 g_A - 6g_A^2)\delta^2 \mathcal{H}_{\eta'}(M_\pi, 0)\}. \quad \text{(B1)}$$

The isovector, unpolarized nucleon matrix element is

$$\langle N|\mathcal{O}_{\mu_0 \cdots \mu_n}^{(3)}|N\rangle = \frac{1}{3}\overline{U}_N v_{\mu_0} \ldots v_{\mu_n} U_N (2\alpha_n^{(a)} - \beta_n^{(a)}) \times [1 + (1 - \delta_{n0})\mathcal{W}_{\text{SU(4|2)}}] + \frac{i(1 - \delta_{n0})}{12f^2}\overline{U}_N v_{\mu_0} \ldots v_{\mu_n} U_N$$

$$\times \left(\frac{4}{3}g_{\Delta N}^2\left(\gamma_n^{(a)} - \frac{\sigma_n^{(a)}}{3}\right) \times [-3\mathcal{H}(M_\pi, \Delta)(-4 + q_j + q_l) + \mathcal{H}(M_{uj}, \Delta)(8 + 3q_j + 3q_l)]\right.$$

$$+ \alpha_n^{(a)}\{-4i\mathcal{I}(M_{uj})(-4 + 3q_j + 3q_l) + 4i\mathcal{I}(M_\pi)(q_j + q_l) + 3[-\mathcal{H}(M_{uj}, 0)(4g_A^2(q_j + q_l)$$

$$+ 2g_1 g_A(2 + q_j + q_l) + g_1^2(6 + q_j + q_l)) + \mathcal{H}(M_\pi, 0)(4g_A^2(1 + q_j + q_l) + 2g_1 g_A(2 + q_j + q_l)$$

$$+ g_1^2(6 + q_j + q_l)) + 8\delta^2(g_1 + g_A)^2 \mathcal{H}_{\eta'}(M_\pi, 0)]\} - \beta_n^{(a)}\{4i\mathcal{I}(M_{uj})(2 + 3q_j + 3q_l)$$

$$- 4i\mathcal{I}(M_\pi)(q_j + q_l) + 3[\mathcal{H}(M_{uj}, 0)g_1(-8g_A + 3g_1(q_j + q_l)) + \mathcal{H}(M_\pi, 0)(8g_1 g_A + 2g_A^2$$

$$- 3g_1^2(q_j + q_l)) + 4\delta^2(g_1 + g_A)^2 \mathcal{H}_{\eta'}(M_\pi, 0)]\}\bigg). \quad \text{(B2)}$$

The isovector, helicity matrix element in the nucleon is

$$
\begin{aligned}
\langle N|\tilde{\mathcal{O}}^{(3)}_{\mu_0\cdots\mu_n}|N\rangle =& \frac{1}{3}\overline{U}_N v_{\{\mu_0}\ldots v_{\mu_{n-1}}S_{\mu_n\}}U_N(2\Delta\alpha_n^{(a)}-\Delta\beta_n^{(a)})\times(1+\mathcal{W}_{\mathrm{SU(4|2)}})+\frac{i}{12f^2}\overline{U}_N v_{\{\mu_0}\ldots v_{\mu_{n-1}}S_{\mu_n\}} \\
& \times U_N\Bigg\{\frac{16}{3}\sqrt{\frac{2}{3}}g_{\Delta N}\Delta c_n^{(a)}[\mathcal{K}(M_\pi,\Delta)(8g_A+g_1(2-3q_j-3q_l))+\mathcal{K}(M_{uj},\Delta)(8g_A+g_1(-2+3q_j+3q_l))] \\
& -\frac{20}{27}g_{\Delta N}^2[3\mathcal{H}(M_\pi,\Delta)(-4+q_j+q_l)-\mathcal{H}(M_{uj},\Delta)(8+3q_j+3q_l)]\left(\Delta\gamma_n^{(a)}-\frac{\Delta\sigma_n^{(a)}}{5}\right) \\
& +\Delta\alpha_n^{(a)}[12i\,I(M_\pi)(q_j+q_l)-4i\,I(M_{uj})(-4+3q_j+3q_l)+\mathcal{H}(M_{uj},0)(4g_A^2(q_j+q_l) \\
& +2g_1g_A(2+q_j+q_l)+g_1^2(6+q_j+q_l))-\mathcal{H}(M_\pi,0)(4g_A^2(1+q_j+q_l)+2g_1g_A(2+q_j+q_l) \\
& +g_1^2(6+q_j+q_l))-8\delta^2(g_1+g_A)^2\mathcal{H}_{\eta'}(M_\pi,0)]+\Delta\beta_n^{(a)}[12i\,I(M_\pi)(q_j+q_l) \\
& -4i\,I(M_{uj})(2+3q_j+3q_l)+\mathcal{H}(M_{uj},0)g_1(-8g_A+3g_1(q_j+q_l))+\mathcal{H}(M_\pi,0)(8g_1g_A+2g_A^2 \\
& -3g_1^2(q_j+q_l))+4\delta^2(g_1+g_A)^2\mathcal{H}_{\eta'}(M_\pi,0)]\Bigg\},
\end{aligned}
\tag{B3}
$$

and the isoscalar, unpolarized matrix element is

$$
\begin{aligned}
\langle N|\mathcal{O}^{(0)}_{\mu_0\cdots\mu_n}|N\rangle =& \overline{U}_N v_{\mu_0}\ldots v_{\mu_n}U_N(\alpha_n^{(s)}+\beta0_n^{(s)})\times[1+(1-\delta_{n0})\mathcal{W}_{\mathrm{SU(4|2)}}]+\frac{i}{2f^2}\overline{U}_N v_{\mu_0}\ldots v_{\mu_n}U_N(1-\delta_{n0}) \\
& \times\Bigg\{4[\mathcal{H}(M_\pi,\Delta)+\mathcal{H}(M_{uj},\Delta)]g_{\Delta N}^2\left(\gamma_n^{(s)}-\frac{\sigma_n^{(s)}}{3}\right)+(\alpha_n^{(s)}+\beta_n^{(s)})[\mathcal{H}(M_\pi,0)(5g_1^2+4g_1g_A-g_A^2) \\
& -\mathcal{H}(M_{uj},0)(5g_1^2+4g_1g_A+8g_A^2)+6\delta^2(g_1+g_A)^2\mathcal{H}_{\eta'}(M_\pi,0)]\Bigg\}.
\end{aligned}
\tag{B4}
$$

The isoscalar, helicity matrix element is

$$
\begin{aligned}
\langle N|\tilde{\mathcal{O}}^{(0)}_{\mu_0\cdots\mu_n}|N\rangle =& \overline{U}_N v_{\{\mu_0}\ldots v_{\mu_{n-1}}S_{\mu_n\}}U_N(\Delta\alpha_n^{(s)}+\Delta\beta_n^{(s)})\times(1+\mathcal{W}_{\mathrm{SU(4|2)}})+\frac{i}{12f^2}\overline{U}_N v_{\{\mu_0}\ldots v_{\mu_{n-1}}S_{\mu_n\}}U_N \\
& \times\Bigg\{\frac{40}{3}[\mathcal{H}(M_\pi,\Delta)+\mathcal{H}(M_{uj},\Delta)]g_{\Delta N}^2\left(\Delta\gamma_n^{(s)}-\frac{\Delta\sigma_n^{(s)}}{5}\right)+(\Delta\alpha_n^{(s)}+\Delta\beta_n^{(s)})[-2\mathcal{H}(M_\pi,0) \\
& \times(5g_1^2+4g_1g_A-g_A^2)+2\mathcal{H}(M_{uj},0)(5g_1^2+4g_1g_A+8g_A^2)-12\delta^2(g_1+g_A)^2\mathcal{H}_{\eta'}(M_\pi,0)]\Bigg\}.
\end{aligned}
\tag{B5}
$$

Finally, the transversity matrix elements are

$$\langle N|\tilde{\mathcal{O}}^T_{\mu_0\cdots\mu_n\alpha}|N\rangle = \frac{1}{6}\overline{U}_N v_{\{\mu_0}\ldots v_{[\mu_n\}}S_{\mu_\alpha]}U_N[(5+y_i)\delta\alpha_n + 2(1+2y_i)\delta\beta_n]\times(1+\mathcal{W}_{SU(4|2)})$$

$$+\frac{i}{12f^2}\overline{U}_N v_{\{\mu_0}\ldots v_{[\mu_n\}}S_{\mu_\alpha]}U_N\left(\frac{16}{3}\sqrt{\frac{2}{3}}g_{\Delta N}\{\mathcal{K}(M_{uj},\Delta)[4g_A(1-y_i)+g_1(-4-2y_i+3y_j+3y_k)]\right.$$

$$+\mathcal{K}(M_\pi,\Delta)[4g_A(1-y_i)+g_1(4+2y_i-3y_l-3y_m)]\}\delta c_n + \frac{20}{27}g^2_{\Delta N}[\mathcal{H}(M_{uj},\Delta)(10+2y_i+3y_j+3y_k)$$

$$+3\mathcal{H}(M_\pi,\Delta)(6+2y_i-y_l-y_m)]\left(\delta\gamma_n-\frac{3\delta\sigma_n}{5}\right)+\delta\alpha_n[2i(I(M_{uj})(10+2y_i+6y_j+6y_k)$$

$$+I(M_\pi)(1+5y_i-6y_l-6y_m))-4(5+y_i)\delta^2 I_{\eta'}(M_\pi)+\mathcal{H}(M_{uj},0)[g_1^2(7+y_i+y_j+y_k)$$

$$+2g_1g_A(2+y_j+y_k)+4g_A^2(1+y_i+y_j+y_k)]+\mathcal{H}(M_\pi,0)[g_A^2(3+7y_i-4y_l-4y_m)$$

$$-2g_1g_A(2+y_l+y_m)-g_1^2(7+y_i+y_l+y_m)]-2(g_1+g_A)^2(5+y_i)\delta^2\mathcal{H}_{\eta'}(M_\pi,0)]$$

$$+\delta\beta_n[4i(I(M_{uj})(2+4y_i+3y_j+3y_k)+I(M_\pi)(2+y_i-3y_l-3y_m))-8(1+2y_i)\delta^2 I_{\eta'}(M_\pi)$$

$$+\mathcal{H}(M_{uj},0)[8g_1g_Ay_i+8g_A^2(1+y_i)+g_1^2(2+2y_i+3y_j+3y_k)]+\mathcal{H}(M_\pi,0)[2g_A^2-8g_1g_Ay_i$$

$$\left.-g_1^2(2+2y_i+3y_l+3y_m)]-4(g_1+g_A)^2(1+2y_i)\delta^2\mathcal{H}_{\eta'}(M_\pi,0)]\right). \tag{B6}$$

APPENDIX C: RESULTS FOR SU(6|3) PQχPT WITH $m_u = m_d \neq m_s$

In three-flavor QCD, one seeks to determine the up, down and strange quark, unpolarized, helicity, and transversity distributions in the octet baryons. Consequently, the goal of lattice calculations is to determine the corresponding twist-two operator matrix elements for each of these flavors in the octet baryons. The SU(6|3) results presented in this appendix will be relevant for chiral and infinite-volume extrapolations of lattice calculations of moments of the strange-quark distributions in the nucleon[6] and the

various parton distributions in, for example, the Λ hyperon [74].

If we consider the extensions of three-flavor QCD to -partially-quenched theories, we are naturally led to SU(6|3) HBχPT. The Lagrangian of this theory is very similar to that described in Sec. II with some simple modifications. Obviously the meson field Φ is enlarged, becoming a 9×9 matrix encoding the **80**-plet of pseudo-Goldstone mesons. The octet baryons are now embedded in a **240** representation and the decuplet baryons in a **138** representation. Additionally, the couplings α, β and C in Eq. (12) are replaced by $\alpha \to \frac{2}{3}D + 2F$, $\beta \to -\frac{5}{3}D + F$ and $C \to C$ so that the nomenclature is the same as in SU(3) χPT. For definiteness, the quark masses we consider are $m_Q = \text{diag}(m_u, m_d, m_s, m_j, m_l, m_r, m_u, m_d, m_s)$ and $\mathcal{Q}$

after Eq. (11) is replaced by $\mathcal{Q} = (u, d, s, j, l, r, \tilde{u}, \tilde{d}, \tilde{s})$. Further details are given in Ref. [42].

To calculate the independent moments of the PDFs in three-flavor QCD, one constructs three independent flavor combinations of operators. The standard choice is

$$i^n\overline{\psi}\Gamma_{\{\mu_0}\overleftrightarrow{D}_{\mu_1}\ldots\overleftrightarrow{D}_{\mu_n\}}\{\mathbf{1},\lambda_3,\lambda_8\}\psi, \tag{C1}$$

where $\Gamma = \gamma, \gamma\gamma_5, \sigma$ represents the appropriate Dirac structure and the λ_i are the usual Gell-Mann basis for SU(3). The unpolarized and helicity operators are in the singlet $(\mathbf{1},\mathbf{1})$ or adjoint $(\mathbf{8},\mathbf{1})\oplus(\mathbf{1},\mathbf{8})$ representations of $SU(3)_L \times SU(3)_R$. From a lattice practitioner's point of view, λ_3 is somewhat special since in the limit $m_u = m_d$ there are no disconnected contributions to matrix elements of such operators. On the other hand, both the singlet and λ_8 operator require such contributions and no choice of flavor basis can ameliorate the situation. In partially-quenched QCD, there is again freedom in the extension of the above QCD operators; a natural choice with a smooth QCD limit is

$$\bar{\lambda}_3 = \text{diag}(1, -1, 0, 1, -1, 0, 1, -1, 0),$$
$$\bar{\lambda}_8 = \text{diag}(1, 1, -2, 1, 1, -2, 1, 1, -2). \tag{C2}$$

In our results, only a single adjoint representation operator is presented, corresponding to

$$\bar{\lambda}_{Adj} = \text{diag}(1, q_1, -1-q_1, 1, q_2, -1-q_2,$$
$$1, q_1, -1-q_1), \tag{C3}$$

and to determine $\bar{\lambda}_3$ and $\bar{\lambda}_8$, we set $q_2 = q_1 = \mp1$. Keeping $q_2 \neq q_1$, will allow SU(3) breaking effects to be analyzed in detail. However, the singlet operator is uniquely defined

---

[6]One can also study strangeness in the nucleon using two-flavor χPT [75] thereby sidestepping issues of the slow(er) convergence of the chiral expansion around the physical strange-quark-mass.

$$\bar{\lambda}_0 = \text{diag}(1, 1, 1, 1, 1, 1, 1, 1, 1) \qquad \text{(C4)}$$

and disconnected loops involving sea quarks are unavoidable.

The transversity operators in QCD belong to the $(\mathbf{3}, \bar{\mathbf{3}}) \oplus (\bar{\mathbf{3}}, \mathbf{3})$ representation of $SU(3)_L \times SU(3)_R$ irrespective of the choice of flavor structure in Eq. (C1). For the partially-quenched QCD extension of these operators, we choose the operators built from

$$\bar{\lambda}_T = \text{diag}(1, y_1, y_2, 0, 0, 0, 1, y_1, y_2) \qquad \text{(C5)}$$

and then setting $\{y_1, y_2\} = \{1, 1\}, \{-1, 0\}, \{1, -2\}$ gives the required flavor combinations.

In this section, we give results for the matrix elements in the proton, Λ^0, Σ^+, Ξ^- as well as the Σ^0–Λ^0 transition. Other octet matrix elements are simply related to these by isospin symmetry. In the results of this section, the low-energy coefficients ($\alpha_n^{(a)}$, $\Delta\gamma_n^{(s)}$, etc) occurring in the SU(6|3) versions of Eqs. (8), (19), and (20) are different from those in SU(4|2). With this caution, we use the same notation.

The SU(6|3) tree-level meson masses, M_{ss}, M_{sr}, M_{ur} and M_{sj}, are defined through Eq. (11), δ is defined in Eq. (24),

$$\tilde{\delta}^2 = M_{ss}^2 - M_{sr}^2 = \lambda(m_s - m_r), \qquad \text{(C6)}$$

and

$$M_X^2 = \frac{1}{3}[M_\pi^2 + 2M_{ss}^2 - 2(\delta^2 + 2\tilde{\delta}^2)]. \qquad \text{(C7)}$$

The QCD limit is easily recovered, taking $\delta \to 0$, $\tilde{\delta} \to 0$, $j \to u$, $l \to d$ and $r \to s$. To make the presentation succinct, we define the following ratios,

$$\mathfrak{A} = -i\frac{\delta^2(M_\pi^2 - M_{ss}^2 + 2\tilde{\delta}^2)}{M_\pi^2 - M_{ss}^2 + \delta^2 + 2\tilde{\delta}^2}, \qquad \text{(C8)}$$

$$\mathfrak{B} = -i\frac{(M_\pi^2 - M_{ss}^2 + 2\tilde{\delta}^2)^2 + 2\delta^4}{2(M_\pi^2 - M_{ss}^2 + \delta^2 + 2\tilde{\delta}^2)^2}, \qquad \text{(C9)}$$

$$\mathfrak{C} = -i\frac{\tilde{\delta}^2(M_\pi^2 - M_{ss}^2 - 2\delta^2)}{M_\pi^2 - M_{ss}^2 - 2\delta^2 - 4\tilde{\delta}^2}, \qquad \text{(C10)}$$

$$\mathfrak{D} = -i\frac{(M_\pi^2 - M_{ss}^2 - 2\delta^2)^2 + 8\tilde{\delta}^4}{M_\pi^2 - M_{ss}^2 - 2\delta^2 - 4\tilde{\delta}^2}, \qquad \text{(C11)}$$

$$\mathfrak{E} = -i\frac{\delta^2(M_\pi^2 - M_{ss}^2 + 2\tilde{\delta}^2)}{(M_\pi^2 - M_{ss}^2)(M_\pi^2 - M_{ss}^2 + \delta^2 + 2\tilde{\delta}^2)}, \qquad \text{(C12)}$$

$$\mathfrak{F} = 2i\frac{\tilde{\delta}^2(M_\pi^2 - M_{ss}^2 - 2\delta^2)}{(M_\pi^2 - M_{ss}^2)(M_\pi^2 - M_{ss}^2 - 2\delta^2 - 4\tilde{\delta}^2)}, \qquad \text{(C13)}$$

and the functions,

$$\begin{aligned}
Q_{uu} &= \mathfrak{A}\, I_{\eta',uu} + \mathfrak{B}\, I_{uu} + (1 - \mathfrak{B})I_X, \\
Q_{ss} &= \mathfrak{C}\, I_{\eta',ss} + \mathfrak{D}\, I_{ss} + (1 - \mathfrak{D})I_X,
\end{aligned} \qquad \text{(C14)}$$

$$\begin{aligned}
R_{uu} &= \mathfrak{A}\, \mathcal{H}_{\eta',uu} + \mathfrak{B}\, \mathcal{H}_{uu} + (1 - \mathfrak{B})\mathcal{H}_X, \\
R_{ss} &= \mathfrak{C}\, \mathcal{H}_{\eta',ss} + \mathfrak{D}\, \mathcal{H}_{ss} + (1 - \mathfrak{D})\mathcal{H}_X, \\
R_{us} &= \mathfrak{E}\, \mathcal{H}_{uu} + \mathfrak{F}\, \mathcal{H}_{ss} + (1 - \mathfrak{E} - \mathfrak{F})\mathcal{H}_X,
\end{aligned} \qquad \text{(C15)}$$

$$\begin{aligned}
S_{uu} &= \mathfrak{A}\, \mathcal{K}_{\eta',uu} + \mathfrak{B}\, \mathcal{K}_{uu} + (1 - \mathfrak{B})\mathcal{K}_X, \\
S_{ss} &= \mathfrak{C}\, \mathcal{K}_{\eta',ss} + \mathfrak{D}\, \mathcal{K}_{ss} + (1 - \mathfrak{D})\mathcal{K}_X, \\
S_{us} &= \mathfrak{E}\, \mathcal{K}_{uu} + \mathfrak{F}\, \mathcal{K}_{ss} + (1 - \mathfrak{E} - \mathfrak{F})\mathcal{K}_X,
\end{aligned} \qquad \text{(C16)}$$

and

$$\begin{aligned}
T_{uu} &= \mathfrak{A}\, \mathcal{H}^\Delta_{\eta',uu} + \mathfrak{B}\, \mathcal{H}^\Delta_{uu} + (1 - \mathfrak{B})\mathcal{H}^\Delta_X, \\
T_{ss} &= \mathfrak{C}\, \mathcal{H}^\Delta_{\eta',ss} + \mathfrak{D}\, \mathcal{H}^\Delta_{ss} + (1 - \mathfrak{D})\mathcal{H}^\Delta_X, \\
T_{us} &= \mathfrak{E}\, \mathcal{H}^\Delta_{uu} + \mathfrak{F}\, \mathcal{H}^\Delta_{ss} + (1 - \mathfrak{E} - \mathfrak{F})\mathcal{H}^\Delta_X,
\end{aligned} \qquad \text{(C17)}$$

where

$$I_{ij} = I(M_{ij}), \qquad I_{\eta',ij} = I_{\eta'}(M_{ij}), \qquad \mathcal{H}_{ij} = \mathcal{H}(M_{ij}, 0), \qquad \mathcal{H}_{\eta',ij} = \mathcal{H}_{\eta'}(M_{ij}, 0), \qquad \mathcal{H}^\Delta_{ij} = \mathcal{H}(M_{ij}, \Delta),$$
$$\mathcal{H}^\Delta_{\eta',ij} = \mathcal{H}_{\eta'}(M_{ij}, \Delta), \qquad \mathcal{K}_{ij} = \mathcal{K}(M_{ij}, \Delta), \qquad \mathcal{K}_{\eta',ij} = \mathcal{K}_{\eta'}(M_{ij}, \Delta), \qquad \text{(C18)}$$

$$I_X = I(M_X), \qquad \mathcal{H}_X = \mathcal{H}(M_X, 0), \qquad \mathcal{H}^\Delta_X = \mathcal{H}(M_X, \Delta), \qquad \mathcal{K}_X = \mathcal{K}(M_X, \Delta), \qquad \text{(C19)}$$

and

$$\begin{aligned}
\mathcal{H}_{abc} &= 2\mathcal{H}(M_{ab}, 0) + \mathcal{H}(M_{ac}, 0), & \hat{\mathcal{H}}_{abc} &= \mathcal{H}(M_{ab}, 0) - \mathcal{H}(M_{ac}, 0), & \mathcal{H}^\Delta_{abc} &= 2\mathcal{H}(M_{ab}, \Delta) + \mathcal{H}(M_{ac}, \Delta), \\
\hat{\mathcal{H}}^\Delta_{abc} &= \mathcal{H}(M_{ab}, \Delta) - \mathcal{H}(M_{ac}, \Delta), & I_{abc} &= 2I(M_{ab}) + I(M_{ac}), & \hat{I}_{abc} &= I(M_{ab}) - I(M_{ac}), \\
\mathcal{K}_{abc} &= 2\mathcal{K}(M_{ab}, \Delta) + \mathcal{K}(M_{ac}, \Delta), & \hat{\mathcal{K}}_{abc} &= \mathcal{K}(M_{ab}, \Delta) - \mathcal{K}(M_{ac}, \Delta),
\end{aligned} \qquad \text{(C20)}$$

and finally

$$\tilde{y} = \frac{y_2}{1 + y_1} \qquad \text{and} \qquad \tilde{q} = \frac{1 + q_2}{1 + q_1}. \tag{C21}$$

1. Wave-function renormalization

The wave-function renormalizations for the different octet states are

$$\mathcal{W}^{(p)}_{\mathrm{SU}(6|3)} = \frac{i}{f^2}\{[2\mathcal{H}^{\Delta}_{uu} + \mathcal{H}^{\Delta}_{ujr}]C^2 + \mathcal{H}_{ujr}(5D^2 - 6DF + 9F^2) - 4\mathcal{H}_{uu}D(D - 3F) - 3iR_{uu}(D - 3F)^2\} \tag{C22}$$

for the proton,

$$\begin{aligned}
\mathcal{W}^{(\Lambda)}_{\mathrm{SU}(6|3)} = \frac{i}{3f^2}\{&3[\mathcal{H}^{\Delta}_{us} + \mathcal{H}^{\Delta}_{uu} + \mathcal{H}^{\Delta}_{ujr}]C^2 + \mathcal{H}_{sjr}(D + 3F)^2 + 2\mathcal{H}_{ujr}(7D^2 - 12DF + 9F^2) \\
&- 2\mathcal{H}_{us}(5D^2 - 6DF - 9F^2) - 2\mathcal{H}_{uu}(D^2 - 12DF + 9F^2) + i[-R_{ss}(3F + D)^2 \\
&+ R_{us}(8D^2 + 12DF - 36F^2) - 4R_{uu}(2D - 3F)^2]\}
\end{aligned} \tag{C23}$$

for the Λ baryons,

$$\begin{aligned}
\mathcal{W}^{(\Sigma)}_{\mathrm{SU}(6|3)} = \frac{i}{3f^2}\{&[5\mathcal{H}^{\Delta}_{us} + \mathcal{H}^{\Delta}_{uu} + 2\mathcal{H}^{\Delta}_{sjr} + \mathcal{H}^{\Delta}_{ujr} - 2i(T_{ss} - 2T_{us} + T_{uu})]C^2 + 3[3\mathcal{H}_{sjr}(D - F)^2 \\
&+ 2\mathcal{H}_{ujr}(D^2 + 3F^2) - 2\mathcal{H}_{uu}(D^2 - 3F^2) - 2\mathcal{H}_{us}(D^2 - 6DF + 3F^2)] - 9i[R_{ss}(D - F)^2 \\
&+ 4R_{us}F(F - D) + 4R_{uu}F^2]\}
\end{aligned} \tag{C24}$$

for the Σ baryons, and

$$\begin{aligned}
\mathcal{W}^{(\Xi)}_{\mathrm{SU}(6|3)} = \frac{i}{3f^2}\{&[5\mathcal{H}^{\Delta}_{us} + \mathcal{H}^{\Delta}_{sjr} + \mathcal{H}^{\Delta}_{ss} + 2\mathcal{H}^{\Delta}_{ujr} - 2i(T_{ss} - 2T_{us} + T_{uu})]C^2 + 3[3\mathcal{H}_{ujr}(D - F)^2 + 2\mathcal{H}_{sjr}(D^2 \\
&+ 3F^2) - 2\mathcal{H}_{us}(D^2 - 6DF + 3F^2) - 2\mathcal{H}_{ss}(D^2 - 3F^2)] - 9i[4R_{ss}F^2 - 4R_{us}F(D - F) + R_{uu}(D - F)^2]\}
\end{aligned} \tag{C25}$$

for the Ξ baryons.

2. Isovector unpolarized matrix elements

$$\begin{aligned}
\langle p|\mathcal{O}^{(3)}_{\mu_0\cdots\mu_n}|p\rangle = &\frac{\overline{U}_p v_{\mu_0}\ldots v_{\mu_n} U_p[(5 + q_1)\alpha_n^{(a)} + 2(1 + 2q_1)\beta_n^{(a)}]}{6} \times [1 + \mathcal{W}^{(p)}_{\mathrm{SU}(6|3)}(1 - \delta_{n0})] \\
&+ \frac{\overline{U}_p v_{\mu_0}\ldots v_{\mu_n} U_p(1 - \delta_{n0})}{f^2}\left(\frac{i}{9}\left(\gamma_n^{(a)} - \frac{\sigma_n^{(a)}}{3}\right)[(3\mathcal{H}^{\Delta}_{uu} + \mathcal{H}^{\Delta}_{ujr})(5 + q_1) + 3(1 + q_2)\hat{\mathcal{H}}^{\Delta}_{ujr}]C^2\right. \\
&+ \alpha_n^{(a)}\left\{\frac{1}{6}(-5 - q_1)I_{ujr} + (1 + q_2)\hat{I}_{ujr} - i\mathcal{H}_{ujr}[3D^2 - 6DF + 5F^2 + (D^2 + F^2)q_1]\right. \\
&+ 4i\mathcal{H}_{uu}D(D - 2F - Fq_1) - i(1 + q_2)(D^2 + 3F^2)\hat{\mathcal{H}}_{ujr} - \frac{1}{2}R_{uu}(D - 3F)^2(5 + q_1)\Big\} \\
&+ \beta_n^{(a)}\left\{\frac{-1}{3}(1 + 2q_1)I_{ujr} + (1 + q_2)\hat{I}_{ujr} - 2i\mathcal{H}_{ujr}[D^2 + F^2(1 + 2q_1)]\right. \\
&+ 4i\mathcal{H}_{uu}D(D - 2F - Fq_1) - 3i(1 + q_2)(D - F)^2\hat{\mathcal{H}}_{ujr} - R_{uu}(D - 3F)^2(1 + 2q_1)\Big\}\bigg).
\end{aligned} \tag{C26}$$

$$
\begin{aligned}
\langle \Lambda^0 | \mathcal{O}^{(3)}_{\mu_0 \cdots \mu_n} | \Lambda^0 \rangle = & -\frac{\overline{U}_{\Lambda^0} v_{\mu_0} \ldots v_{\mu_n} U_{\Lambda^0}(1+q_1)}{4}(\alpha_n^{(a)} - 2\beta_n^{(a)}) \times [1 + \mathcal{W}^{(\Lambda)}_{\mathrm{SU}(6|3)}(1 - \delta_{n0})] \\
& + \frac{\overline{U}_{\Lambda^0} v_{\mu_0} \ldots v_{\mu_n} U_{\Lambda^0}(1+q_1)(1 - \delta_{n0})}{f^2}\bigg(-\frac{i}{6}\bigg(\gamma_n^{(a)} - \frac{\sigma_n^{(a)}}{3}\bigg)(3\mathcal{H}^\Delta_{us} + \mathcal{H}^\Delta_{ujr} - 2\tilde{q}\hat{\mathcal{H}}^\Delta_{ujr})C^2 \\
& + \alpha_n^{(a)}\bigg\{\frac{1}{4}(-I_{ujr} + 2I_{sjr}) + \frac{\tilde{q}}{2}(\hat{I}_{ujr} + \hat{I}_{sjr}) + \frac{i}{12}\mathcal{H}_{ujr}(7D - 9F)(D - 3F) \\
& - \frac{i}{12}\mathcal{H}_{sjr}(D + 3F)^2 - \frac{i}{6}\mathcal{H}_{uu}(7D^2 - 12DF + 9F^2) - \frac{i}{6}\mathcal{H}_{us}(5D - 3F)(D + 3F) \\
& - \frac{i}{6}\tilde{q}(D + 3F)^2\hat{\mathcal{H}}_{sjr} - \frac{i}{6}\tilde{q}(5D^2 - 6DF + 9F^2)\hat{\mathcal{H}}_{ujr} + \frac{1}{12}[R_{ss}(D + 3F)^2 \\
& - 4R_{us}(2D - 3F)(D + 3F) + 4R_{uu}(2D - 3F)^2]\bigg\} + \beta_n^{(a)}\bigg\{-\frac{1}{2}(2I_{uj} + I_{ur}) + \tilde{q}\hat{I}_{ujr} \\
& + \frac{i}{6}\mathcal{H}_{ujr}(7D^2 + 6DF - 9F^2) - \frac{i}{6}\mathcal{H}_{sjr}(D + 3F)^2 - \frac{i}{3}\mathcal{H}_{uu}(7D^2 - 12DF + 9F^2) \\
& - \frac{i}{3}\mathcal{H}_{us}(13D^2 - 12DF + 9F^2) - 3i\tilde{q}(D - F)^2\hat{\mathcal{H}}_{ujr} - \frac{1}{6}[R_{ss}(D + 3F)^2 \\
& - 4R_{us}(2D - 3F)(D + 3F) + 4R_{uu}(2D - 3F)^2]\bigg\}\bigg).
\end{aligned}
\tag{C27}
$$

$$
\begin{aligned}
\langle \Sigma^+ | \mathcal{O}^{(3)}_{\mu_0 \cdots \mu_n} | \Sigma^+ \rangle = & -\frac{\overline{U}_{\Sigma^+} v_{\mu_0} \ldots v_{\mu_n} U_{\Sigma^+}[(-4 + q_1)\alpha_n^{(a)} + 2(1 + 2q_1)\beta_n^{(a)}]}{6} \times [1 + \mathcal{W}^{(\Sigma)}_{\mathrm{SU}(6|3)}(1 - \delta_{n0})] \\
& + \frac{\overline{U}_{\Sigma^+} v_{\mu_0} \ldots v_{\mu_n} U_{\Sigma^+}(1 - \delta_{n0})}{f^2}\bigg(\frac{i}{9}\bigg(\gamma_n^{(a)} - \frac{\sigma_n^{(a)}}{3}\bigg)[\mathcal{H}^\Delta_{uu} + 11\mathcal{H}^\Delta_{us} + 4\mathcal{H}^\Delta_{sjr} - [\mathcal{H}^\Delta_{uu} + 2\mathcal{H}^\Delta_{us} \\
& + \mathcal{H}^\Delta_{ujr}]q_1 + (1 + q_2)(\hat{\mathcal{H}}^\Delta_{ujr} + 2\hat{\mathcal{H}}^\Delta_{sjr}) - 2i(T_{ss} - 2T_{us} + T_{uu})(1 - q_1)]C^2 \\
& + \alpha_n^{(a)}\bigg\{\frac{1}{6}[-5I_{ujr} + I_{sjr}(1 + q_1) + (1 + q_2)(5\hat{I}_{ujr} + \hat{I}_{sjr})] + \frac{i}{2}\mathcal{H}_{ujr}[(D - F)(D + 3F) \\
& + 2(D^2 + F^2)q_1] - \frac{5i}{2}\mathcal{H}_{sjr}(D - F)^2 - i\mathcal{H}_{uu}[4F^2 + (D - F)(D + F)q_1] \\
& + i\mathcal{H}_{us}[4(D^2 - DF + F^2) + (D^2 + 4DF - F^2)q_1] - \frac{i}{2}(1 + q_2)(D^2 + 2DF + 5F^2)\hat{\mathcal{H}}_{ujr} \\
& - \frac{i}{2}(1 + q_2)(D - F)^2\hat{\mathcal{H}}_{sjr} + \frac{1}{2}[R_{ss}(D - F)^2 - 4R_{us}F(D - F) + 4R_{uu}F^2](q_1 - 4)\bigg\} \\
& + \beta_n^{(a)}\bigg\{\frac{1}{3}[-I_{ujr} + 2I_{sjr}(1 + q_1) + (1 + q_2)(\hat{I}_{ujr} + 2\hat{I}_{sjr})] - i\mathcal{H}_{ujr}[(D - F)(D + 3F) - 4F^2q_1] \\
& - i\mathcal{H}_{sjr}(D - F)^2 + 2i\mathcal{H}_{uu}(D^2 + F^2 + 2F^2q_1) + 2i\mathcal{H}_{us}[D^2 - 2DF - F^2 + 2(D - F)Fq_1] \\
& - i(1 + q_2)(D - F)^2(\hat{\mathcal{H}}_{ujr} + 2\hat{\mathcal{H}}_{sjr}) + [R_{ss}(D - F)^2 - 4R_{us}F(D - F) + 4R_{uu}F^2](1 + 2q_1)\bigg\}\bigg).
\end{aligned}
\tag{C28}
$$

$$\langle \Xi^- | \mathcal{O}^{(3)}_{\mu_0 \cdots \mu_n} | \Xi^- \rangle = -\frac{\overline{U}_{\Xi^-} v_{\mu_0} \ldots v_{\mu_n} U_{\Xi^-} [(5 + 4q_1)\alpha_n^{(a)} - 2(-1 + q_1)\beta_n^{(a)}]}{6} \times [1 + \mathcal{W}^{(\Xi)}_{SU(6|3)}(1 - \delta_{n0})]$$

$$+ \frac{\overline{U}_{\Xi^-} v_{\mu_0} \ldots v_{\mu_n} U_{\Xi^-}(1 - \delta_{n0})}{f^2}\left(-\frac{i}{9}\left(\gamma_n^{(a)} - \frac{\sigma_n^{(a)}}{3}\right)[\mathcal{H}^\Delta_{sjr} + \mathcal{H}^\Delta_{ss}(2 + q_1) + \mathcal{H}^\Delta_{us}(13 + 11q_1)\right.$$

$$+ 4\mathcal{H}^\Delta_{ujr}(1 + q_1) - (1 + q_2)(2\hat{\mathcal{H}}^\Delta_{ujr} + \hat{\mathcal{H}}^\Delta_{sjr}) - 2i(T_{ss} - 2T_{us} + T_{uu})(2 + q_1)]C^2$$

$$+ \alpha_n^{(a)}\left\{\frac{1}{6}[-I_{ujr}q_1 + 5I_{sjr}(1 + q_1) + (1 + q_2)(\hat{I}_{ujr} + 5\hat{I}_{sjr})] + \frac{5i}{2}\mathcal{H}_{ujr}(D - F)^2(1 + q_1)\right.$$

$$+ \frac{i}{2}\mathcal{H}_{sjr}[D^2 - 2DF + 5F^2 - (D - F)(D + 3F)q_1] - i\mathcal{H}_{ss}(D^2 - 5F^2 - 4F^2 q_1)$$

$$- i\mathcal{H}_{us}[(3D - 5F)(D - F) + 4(D^2 - DF + F^2)q_1] - \frac{i}{2}(1 + q_2)(D - F)^2\hat{\mathcal{H}}_{ujr}$$

$$\left. - \frac{i}{2}(1 + q_2)(D^2 + 2DF + 5F^2)\hat{\mathcal{H}}_{sjr} + \frac{1}{2}[4R_{ss}F^2 - 4R_{us}F(D - F) + R_{uu}(D - F)^2](5 + 4q_1)\right\}$$

$$+ \beta_n^{(a)}\left\{\frac{1}{3}[-2I_{ujr}q_1 + I_{sjr}(1 + q_1) + (1 + q_2)(2\hat{I}_{ujr} + \hat{I}_{sjr})] + i\mathcal{H}_{sjr}[(D + F)^2\right.$$

$$+ (D - F)(D + 3F)q_1] - 2i\mathcal{H}_{ss}[D^2 - F^2 + (D^2 + F^2)q_1] - 2i\mathcal{H}_{us}[D^2 - 4DF + F^2$$

$$+ (D^2 - 2DF - F^2)q_1] - i(1 + q_2)(D - F)^2(2\hat{\mathcal{H}}_{ujr} + \hat{\mathcal{H}}_{sjr}) + i\mathcal{H}_{ujr}[(D - F)^2(1 + q_1)]$$

$$\left.\left. + [4R_{ss}F^2 - 4R_{us}F(D - F) + R_{uu}(D - F)^2](1 - q_1)\right\}\right). \tag{C29}$$

$$\langle \Sigma^0 | \mathcal{O}^{(3)}_{\mu_0 \cdots \mu_n} | \Lambda^0 \rangle = -\frac{\overline{U}_{\Sigma^0} v_{\mu_0} \ldots v_{\mu_n} U_{\Lambda^0}(-1 + q_1)}{4\sqrt{3}}(\alpha_n^{(a)} - 2\beta_n^{(a)}) \times \left[1 + \frac{1}{2}(\mathcal{W}^{(\Lambda)}_{SU(6|3)} + \mathcal{W}^{(\Sigma)}_{SU(6|3)})(1 - \delta_{n0})\right]$$

$$+ \frac{\overline{U}_{\Sigma^0} v_{\mu_0} \ldots v_{\mu_n} U_{\Lambda^0}(-1 + q_1)(1 - \delta_{n0})}{\sqrt{3}f^2}\left(-\frac{i}{6}\left(\gamma_n^{(a)} - \frac{\sigma_n^{(a)}}{3}\right)(2\mathcal{H}^\Delta_{uu} + \mathcal{H}^\Delta_{us} + \mathcal{H}^\Delta_{ujr})C^2\right.$$

$$+ \alpha_n^{(a)}\left\{\frac{1}{4}I_{ujr} + \frac{i}{4}\mathcal{H}_{ujr}(D - 3F)(3D - F) - \frac{i}{4}\mathcal{H}_{sjr}(D - F)(D + 3F) - i\mathcal{H}_{uu}D(D + F)\right.$$

$$\left. - i\mathcal{H}_{us}D(D - F) - \frac{1}{4}[R_{ss}(D - F)(D + 3F) - 4R_{us}(D^2 - 2DF + 3F^2) - 4R_{uu}F(-2D + 3F)]\right\}$$

$$+ \beta_n^{(a)}\left\{-\frac{1}{2}I_{ujr} + \frac{i}{2}\mathcal{H}_{ujr}(D - 3F)(D + F) + \frac{i}{2}\mathcal{H}_{sjr}(D - F)(D + 3F) - 2i\mathcal{H}_{uu}D(D - F)\right.$$

$$\left.\left. - 2i\mathcal{H}_{us}DF + \frac{1}{2}[R_{ss}(D - F)(D + 3F) - 4R_{us}(D^2 - 2DF + 3F^2) - 4R_{uu}F(-2D + 3F)]\right\}\right). \tag{C30}$$

3. Isovector helicity matrix elements

$$\langle p|\tilde{\mathcal{O}}^{(3)}_{\mu_0\cdots\mu_n}|p\rangle = \frac{\overline{U}_p v_{\{\mu_0}\ldots v_{\mu_{n-1}} S_{\mu_n\}} U_p[(5+q_1)\Delta\alpha_n^{(a)} + 2(1+2q_1)\Delta\beta_n^{(a)}]}{6} \times (1 + \mathcal{W}^{(p)}_{\mathrm{SU}(6|3)})$$

$$+ \frac{\overline{U}_p v_{\{\mu_0}\ldots v_{\mu_{n-1}} S_{\mu_n\}} U_p}{f^2}\left(\frac{5i}{81}\left(\Delta\gamma_n^{(a)} - \frac{\Delta\sigma_n^{(a)}}{5}\right)[(3\mathcal{H}^{\Delta}_{uu} + \mathcal{H}^{\Delta}_{ujr})(5+q_1)\right.$$

$$+ 3(1+q_2)\hat{\mathcal{H}}^{\Delta}_{ujr}]C^2 + \frac{8i}{9}\sqrt{\frac{2}{3}}[\mathcal{K}_{uu}(D+3F)(-1+q_1) - \mathcal{K}_{ujr}(3D-F-2Fq_1)$$

$$+ 3(1+q_2)(D-F)\hat{\mathcal{K}}_{ujr}]C\Delta c_n^{(a)} + \Delta\alpha_n^{(a)}\left\{-\frac{1}{6}(5+q_1)I_{ujr} + (1+q_2)\hat{I}_{ujr} + \frac{i}{3}\mathcal{H}_{ujr}[3D^2 - 6DF\right.$$

$$+ 5F^2 + (D^2+F^2)q_1] - \frac{4i}{3}\mathcal{H}_{uu}D(D-2F-Fq_1) + \frac{i}{3}(1+q_2)(D^2+3F^2)\hat{\mathcal{H}}_{ujr}$$

$$\left.+ \frac{1}{6}R_{uu}(D-3F)^2(5+q_1)\right\} + \Delta\beta_n^{(a)}\left\{-\frac{1}{3}(1+2q_1)I_{ujr} + (1+q_2)\hat{I}_{ujr}\right.$$

$$+ \frac{2i}{3}\mathcal{H}_{ujr}[D^2+F^2(1+2q_1)] - \frac{4i}{3}\mathcal{H}_{uu}D(D-2F-Fq_1) + i(1+q_2)(D-F)^2\hat{\mathcal{H}}_{ujr}$$

$$\left.\left.+ \frac{1}{3}R_{uu}(D-3F)^2(1+2q_1)\right\}\right). \tag{C31}$$

$$\langle\Lambda^0|\tilde{\mathcal{O}}^{(3)}_{\mu_0\cdots\mu_n}|\Lambda^0\rangle = -\frac{\overline{U}_{\Lambda^0} v_{\{\mu_0}\ldots v_{\mu_{n-1}} S_{\mu_n\}} U_{\Lambda^0}(1+q_1)}{4}(\Delta\alpha_n^{(a)} - 2\Delta\beta_n^{(a)}) \times (1 + \mathcal{W}^{(\Lambda)}_{\mathrm{SU}(6|3)})$$

$$+ \frac{\overline{U}_{\Lambda^0} v_{\{\mu_0}\ldots v_{\mu_{n-1}} S_{\mu_n\}} U_{\Lambda^0}(1+q_1)}{f^2}\left(-\frac{5i}{54}\left(\Delta\gamma_n^{(a)} - \frac{\Delta\sigma_n^{(a)}}{5}\right)(3\mathcal{H}^{\Delta}_{us} + \mathcal{H}^{\Delta}_{ujr} - 2\tilde{q}\hat{\mathcal{H}}^{\Delta}_{ujr})C^2\right.$$

$$+ \frac{4i}{3}\sqrt{\frac{2}{3}}[-\mathcal{K}_{us}(D-3F) + 2\mathcal{K}_{uu}D + \mathcal{K}_{ujr}(D+F) + 2\tilde{q}(D-F)\hat{\mathcal{K}}_{ujr}]C\Delta c_n^{(a)}$$

$$+ \Delta\alpha_n^{(a)}\left\{\frac{1}{4}[-I_{ujr} + 2I_{sjr} + 2\tilde{q}(\hat{I}_{ujr} + \hat{I}_{sjr})] - \frac{i}{36}\mathcal{H}_{ujr}(7D-9F)(D-3F)\right.$$

$$+ \frac{i}{36}\mathcal{H}_{sjr}(D+3F)^2 + \frac{i}{18}\mathcal{H}_{uu}(7D^2 - 12DF + 9F^2) + \frac{i}{18}\mathcal{H}_{us}(5D-3F)(D+3F)$$

$$+ \frac{i}{18}\tilde{q}(5D^2 - 6DF + 9F^2)\hat{\mathcal{H}}_{ujr} + \frac{i}{18}\tilde{q}(D+3F)^2\hat{\mathcal{H}}_{sjr} - \frac{1}{36}[R_{ss}(D+3F)^2$$

$$\left.- 4R_{us}(2D-3F)(D+3F) + 4R_{uu}(2D-3F)^2]\right\} + \Delta\beta_n^{(a)}\left\{-\frac{1}{2}I_{ujr} + \tilde{q}\hat{I}_{ujr}\right.$$

$$- \frac{i}{18}\mathcal{H}_{ujr}(7D^2 + 6DF - 9F^2) + \frac{i}{18}\mathcal{H}_{sjr}(D+3F)^2 - \frac{i}{9}\mathcal{H}_{uu}(7D^2 - 12DF + 9F^2)$$

$$+ \frac{i}{9}\mathcal{H}_{us}(13D^2 - 12DF + 9F^2) + i\tilde{q}(D-F)^2\hat{\mathcal{H}}_{ujr} + \frac{1}{18}[R_{ss}(D+3F)^2$$

$$\left.\left.- 4R_{us}(2D-3F)(D+3F) + 4R_{uu}(2D-3F)^2]\right\}\right). \tag{C32}$$

$$\langle\Sigma^+|\tilde{\mathcal{O}}^{(3)}_{\mu_0\cdots\mu_n}|\Sigma^+\rangle = -\frac{\overline{U}_{\Sigma^+}v_{\{\mu_0}\ldots v_{\mu_{n-1}}S_{\mu_n\}}U_{\Sigma^+}[(-4+q_1)\Delta\alpha_n^{(a)}+2(1+2q_1)\Delta\beta_n^{(a)}]}{6}\times(1+\mathcal{W}^{(\Sigma)}_{\text{SU}(6|3)})$$

$$+\frac{\overline{U}_{\Sigma^+}v_{\{\mu_0}\ldots v_{\mu_{n-1}}S_{\mu_n\}}U_{\Sigma^+}}{f^2}\left\{\frac{5i}{81}\left(\Delta\gamma_n^{(a)}-\frac{\Delta\sigma_n^{(a)}}{5}\right)(\mathcal{H}^\Delta_{uu}+11\mathcal{H}^\Delta_{us}+4\mathcal{H}^\Delta_{sjr}\right.$$

$$-[\mathcal{H}^\Delta_{uu}+2\mathcal{H}^\Delta_{us}+\mathcal{H}^\Delta_{ujr}]q_1+(1+q_2)(\hat{\mathcal{H}}^\Delta_{ujr}+2\hat{\mathcal{H}}^\Delta_{sjr})-2i(T_{ss}-2T_{us}+T_{uu})(1-q_1))C^2$$

$$-\frac{8i}{9}\sqrt{\frac{2}{3}}[\mathcal{K}_{ujr}(D+3F+2Fq_1)+2\mathcal{K}_{sjr}(D-F)+2\mathcal{K}_{uu}F(2+q_1)+\mathcal{K}_{us}(D+F)(2+q_1)$$

$$+(1+q_2)(F-D)(\hat{\mathcal{K}}_{ujr}+2\hat{\mathcal{K}}_{sjr})-2i(S_{ss}(D-F)+2S_{uu}F-S_{us}(D+F))(2+q_1)]C\Delta c_n^{(a)}$$

$$+\Delta\alpha_n^{(a)}\left[\frac{1}{6}(-5I_{ujr}+I_{sjr}(1+q_1)+(1+q_2)(5\hat{I}_{ujr}+\hat{I}_{sjr}))-\frac{i}{6}\mathcal{H}_{ujr}((D-F)(D+3F)\right.$$

$$+2(D^2+F^2)q_1)+\frac{5i}{6}\mathcal{H}_{sjr}(D-F)^2+\frac{i}{3}\mathcal{H}_{uu}(4F^2+(D-F)(D+F)q_1)$$

$$-\frac{i}{3}\mathcal{H}_{us}(4(D^2-DF+F^2)+(D^2+4DF-F^2)q_1)+\frac{i}{6}(1+q_2)(D^2+2DF+5F^2)\hat{\mathcal{H}}_{ujr}$$

$$+\frac{i}{6}(1+q_2)(D-F)^2\hat{\mathcal{H}}_{sjr}-\frac{1}{6}(R_{ss}(D-F)^2-4R_{us}F(D-F)+4R_{uu}F^2)(q_1-4)]$$

$$+\Delta\beta_n^{(a)}\left[\frac{1}{3}(-I_{ujr}+2I_{sjr}(1+q_1)+(1+q_2)(\hat{I}_{ujr}+2\hat{I}_{sjr})))+\frac{i}{3}\mathcal{H}_{ujr}((D-F)(D+3F)\right.$$

$$-4F^2q_1)+\frac{i}{3}\mathcal{H}_{sjr}(D-F)^2-\frac{2i}{3}\mathcal{H}_{uu}(D^2+F^2+2F^2q_1)-\frac{2i}{3}\mathcal{H}_{us}(D^2-2DF$$

$$-F^2+2(D-F)Fq_1)+\frac{i}{3}(1+q_2)(D-F)^2(\hat{\mathcal{H}}_{ujr}+2\hat{\mathcal{H}}_{sjr})-\frac{1}{3}(R_{ss}(D-F)^2-4R_{us}F(D-F)$$

$$\left.\left.+4R_{uu}F^2)(1+2q_1)\right]\right\}. \tag{C33}$$

$$
\langle \Xi^- | \tilde{\mathcal{O}}^{(3)}_{\mu_0 \cdots \mu_n} | \Xi^- \rangle = - \frac{\overline{U}_{\Xi^-} v_{\{\mu_0} \ldots v_{\mu_{n-1}} S_{\mu_n\}} U_{\Xi^-} [(5 + 4q_1) \Delta \alpha_n^{(a)} - 2(-1 + q_1) \Delta \beta_n^{(a)}]}{6} \times (1 + \mathcal{W}^{(\Xi)}_{\mathrm{SU}(6|3)})
$$

$$
+ \frac{\overline{U}_{\Xi^-} v_{\{\mu_0} \ldots v_{\mu_{n-1}} S_{\mu_n\}} U_{\Xi^-}}{f^2} \left\{ -\frac{5i}{81} \left(\Delta \gamma_n^{(a)} - \frac{\Delta \sigma_n^{(a)}}{5} \right) (\mathcal{H}^\Delta_{sjr} + \mathcal{H}^\Delta_{ss}(2 + q_1) + \mathcal{H}^\Delta_{us}(13 + 11q_1) \right.
$$

$$
+ 4\mathcal{H}^\Delta_{ujr}](1 + q_1) - (1 + q_2)(2\hat{\mathcal{H}}^\Delta_{ujr} + \hat{\mathcal{H}}^\Delta_{sjr}) - 2i(T_{ss} - 2T_{us} + T_{uu})(2 + q_1))C^2
$$

$$
+ \frac{8i}{9}\sqrt{\frac{2}{3}}[2\mathcal{K}_{ujr}(D - F)(1 + q_1) + \mathcal{K}_{sjr}(D + F + (D + 3F)q_1) + 2\mathcal{K}_{ss}F(1 + 2q_1)
$$

$$
+ \mathcal{K}_{us}(D + F)(1 + 2q_1) + (1 + q_2)(D - F)(2\hat{\mathcal{K}}_{ujr} + \hat{\mathcal{K}}_{sjr}) - 2i(S_{uu}(D - F) + 2S_{ss}F
$$

$$
- S_{us}(D + F))(1 + 2q_1)]C\Delta c_n^{(a)} + \Delta \alpha_n^{(a)}\left[\frac{1}{6}(-I_{ujr}q_1 + 5I_{sjr}(1 + q_1) + (1 + q_2)(\hat{I}_{ujr} + 5\hat{I}_{sjr})) \right.
$$

$$
- \frac{5i}{6}\mathcal{H}_{ujr}(D - F)^2(1 + q_1) - \frac{i}{6}\mathcal{H}_{sjr}(D^2 - 2DF + 5F^2 - (D - F)(D + 3F)q_1)
$$

$$
+ \frac{i}{3}\mathcal{H}_{ss}(D^2 - 5F^2 - 4F^2 q_1) + \frac{i}{3}\mathcal{H}_{us}((3D - 5F)(D - F) + 4(D^2 - DF + F^2)q_1)
$$

$$
+ \frac{i}{6}(1 + q_2)(D - F)^2 \hat{\mathcal{H}}_{ujr} + \frac{i}{6}(1 + q_2)(D^2 + 2DF + 5F^2)\hat{\mathcal{H}}_{sjr} - \frac{1}{6}(4R_{ss}F^2 - 4R_{us}F(D - F)
$$

$$
\left. + R_{uu}(D - F)^2)(5 + 4q_1) \right] + \Delta \beta_n^{(a)}\left[\frac{1}{3}(-2I_{ujr}q_1 + I_{sjr}(1 + q_1) + (1 + q_2)(2\hat{I}_{ujr} + \hat{I}_{sjr})) \right.
$$

$$
- \frac{i}{3}\mathcal{H}_{ujr}(D - F)^2(1 + q_1) - \frac{i}{3}\mathcal{H}_{sjr}((D + F)^2 + (D - F)(D + 3F)q_1)
$$

$$
+ \frac{2i}{3}\mathcal{H}_{ss}(D^2 - F^2 + (D^2 + F^2)q_1) + \frac{i}{3}(1 + q_2)(D - F)^2(2\hat{\mathcal{H}}_{ujr} + \hat{\mathcal{H}}_{sjr}) + \frac{2i}{3}\mathcal{H}_{us}(D^2 - 4DF
$$

$$
\left. \left. + F^2 + (D^2 - 2DF - F^2)q_1) - \frac{1}{3}(4R_{ss}F^2 - 4R_{us}F(D - F) + R_{uu}(D - F)^2)(1 - q_1) \right] \right\}. \quad \text{(C34)}
$$

$$
\langle \Sigma^0 | \tilde{\mathcal{O}}^{(3)}_{\mu_0 \cdots \mu_n} | \Lambda^0 \rangle = - \frac{\overline{U}_{\Sigma^0} v_{\{\mu_0} \ldots v_{\mu_{n-1}} S_{\mu_n\}} U_{\Lambda^0}(-1 + q_1)}{4\sqrt{3}} (\Delta \alpha_n^{(a)} - 2\Delta \beta_n^{(a)}) \times \left[1 + \frac{1}{2}(\mathcal{W}^{(\Lambda)}_{\mathrm{SU}(6|3)} + \mathcal{W}^{(\Sigma)}_{\mathrm{SU}(6|3)}) \right]
$$

$$
+ \frac{\overline{U}_{\Sigma^0} v_{\{\mu_0} \ldots v_{\mu_{n-1}} S_{\mu_n\}} U_{\Lambda^0}(-1 + q_1)}{\sqrt{3}f^2} \left(-\frac{5i}{54} \left(\Delta \gamma_n^{(a)} - \frac{\Delta \sigma_n^{(a)}}{5} \right)(2\mathcal{H}^\Delta_{uu} + \mathcal{H}^\Delta_{us} + \mathcal{H}^\Delta_{ujr})C^2 \right.
$$

$$
+ \frac{4i}{9}\sqrt{\frac{2}{3}}\{2\mathcal{K}_{us}(2D + 3F) - \mathcal{K}_{uu}(D - 3F) + 2\mathcal{K}_{ujr}D + \mathcal{K}_{sjr}(D + 3F) - i[2S_{uu}(2D - 3F)
$$

$$
+ S_{us}(-5D + 3F) + S_{ss}(D + 3F)]\}C\Delta c_n^{(a)} + \Delta \alpha_n^{(a)}\left\{ \frac{1}{4}I_{ujr} - \frac{i}{12}\mathcal{H}_{ujr}(D - 3F)(3D - F) \right.
$$

$$
+ \frac{i}{12}\mathcal{H}_{sjr}(D - F)(D + 3F) + \frac{i}{3}\mathcal{H}_{uu}D(D + F) + \frac{i}{3}\mathcal{H}_{us}D(D - F) + \frac{1}{12}[R_{ss}(D - F)(D + 3F)
$$

$$
\left. - 4R_{us}(D^2 - 2DF + 3F^2) - 4R_{uu}F(-2D + 3F)] \right\} + \Delta \beta_n^{(a)}\left\{ -\frac{1}{2}I_{ujr} - \frac{i}{6}\mathcal{H}_{ujr}(D - 3F)(D + F) \right.
$$

$$
- \frac{i}{6}\mathcal{H}_{sjr}(D - F)(D + 3F) + \frac{2i}{3}\mathcal{H}_{uu}D(D - F) + \frac{2i}{3}\mathcal{H}_{us}DF - \frac{1}{6}[R_{ss}(D - F)(D + 3F)
$$

$$
\left. \left. - 4R_{us}(D^2 - 2DF + 3F^2) - 4R_{uu}F(-2D + 3F)]\} \right). \quad \text{(C35)}
$$

4. Isoscalar unpolarized matrix elements

$$\langle p|\mathcal{O}^{(0)}_{\mu_0\cdots\mu_n}|p\rangle = \overline{U}_p v_{\mu_0}\ldots v_{\mu_n} U_p(\alpha_n^{(s)} + \beta_n^{(s)}) \times [1 + (1-\delta_{n0})\mathcal{W}^{(p)}_{\mathrm{SU(6|3)}}] + \frac{\overline{U}_p v_{\mu_0}\ldots v_{\mu_n} U_p(1-\delta_{n0})}{f^2}$$

$$\times \left\{ i\left(\gamma_n^{(s)} - \frac{\sigma_n^{(s)}}{3}\right)(2\mathcal{H}^\Delta_{uu} + \mathcal{H}^\Delta_{ujr})C^2 + (\alpha_n^{(s)} + \beta_n^{(s)})[-i\mathcal{H}_{ujr}(5D^2 - 6DF + 9F^2) \right.$$

$$\left. + 4i\mathcal{H}_{uu}D(D-3F) - 3R_{uu}(D-3F)^2] \right\}. \tag{C36}$$

$$\langle \Lambda^0|\mathcal{O}^{(0)}_{\mu_0\cdots\mu_n}|\Lambda^0\rangle = \overline{U}_{\Lambda^0} v_{\mu_0}\ldots v_{\mu_n} U_{\Lambda^0}(\alpha_n^{(s)} + \beta_n^{(s)}) \times [1 + (1-\delta_{n0})\mathcal{W}^{(\Lambda)}_{\mathrm{SU(6|3)}}] + \frac{\overline{U}_{\Lambda^0} v_{\mu_0}\ldots v_{\mu_n} U_{\Lambda^0}(1-\delta_{n0})}{f^2}$$

$$\times \left(i\left(\gamma_n^{(s)} - \frac{\sigma_n^{(s)}}{3}\right)(\mathcal{H}^\Delta_{us} + \mathcal{H}^\Delta_{uu} + \mathcal{H}^\Delta_{ujr})C^2 + (\alpha_n^{(s)} + \beta_n^{(s)})\left\{-\frac{2i}{3}\mathcal{H}_{ujr}(7D^2 - 12DF + 9F^2) \right.\right.$$

$$\left.\left. - \frac{i}{3}\mathcal{H}_{sjr}(D+3F)^2 + \frac{2i}{3}\mathcal{H}_{uu}(D^2 - 12DF + 9F^2) + \frac{2i}{3}\mathcal{H}_{us}(5D^2 - 6DF - 9F^2) \right.\right.$$

$$\left.\left. - \frac{1}{3}[R_{ss}(D+3F)^2 - 4R_{us}(2D-3F)(D+3F) + 4R_{uu}(2D-3F)^2] \right\} \right). \tag{C37}$$

$$\langle \Sigma^+|\mathcal{O}^{(0)}_{\mu_0\cdots\mu_n}|\Sigma^+\rangle = \overline{U}_{\Sigma^+} v_{\mu_0}\ldots v_{\mu_n} U_{\Sigma^+}(\alpha_n^{(s)} + \beta_n^{(s)}) \times [1 + (1-\delta_{n0})\mathcal{W}^{(\Sigma)}_{\mathrm{SU(6|3)}}] + \frac{\overline{U}_{\Sigma^+} v_{\mu_0}\ldots v_{\mu_n} U_{\Sigma^+}(1-\delta_{n0})}{f^2}$$

$$\times \left(\frac{i}{3}\left(\gamma_n^{(s)} - \frac{\sigma_n^{(s)}}{3}\right)[\mathcal{H}^\Delta_{uu} + 5\mathcal{H}^\Delta_{us} + 2\mathcal{H}^\Delta_{sjr} + \mathcal{H}^\Delta_{ujr} - 2i(T_{ss} - 2T_{us} + T_{uu})]C^2 \right.$$

$$\left. + (\alpha_n^{(s)} + \beta_n^{(s)})\{-2i\mathcal{H}_{ujr}(D^2 + 3F^2) - 3i\mathcal{H}_{sjr}(D-F)^2 + 2i\mathcal{H}_{uu}(D^2 - 3F^2) \right.$$

$$\left. + 2i\mathcal{H}_{us}(D^2 - 6DF + 3F^2) - 3[R_{ss}(D-F)^2 - 4R_{us}F(D-F) + 4R_{uu}F^2]\} \right). \tag{C38}$$

$$\langle \Xi^-|\mathcal{O}^{(0)}_{\mu_0\cdots\mu_n}|\Xi^-\rangle = \overline{U}_{\Xi^-} v_{\mu_0}\ldots v_{\mu_n} U_{\Xi^-}(\alpha_n^{(s)} + \beta_n^{(s)}) \times [1 + (1-\delta_{n0})\mathcal{W}^{(\Xi)}_{\mathrm{SU(6|3)}}] + \frac{\overline{U}_{\Xi^-} v_{\mu_0}\ldots v_{\mu_n} U_{\Xi^-}(1-\delta_{n0})}{f^2}$$

$$\times \left(\frac{i}{3}\left(\gamma_n^{(s)} - \frac{\sigma_n^{(s)}}{3}\right)[2\mathcal{H}^\Delta_{ujr} + \mathcal{H}^\Delta_{sjr} + \mathcal{H}^\Delta_{ss} + 5\mathcal{H}^\Delta_{us} - 2i(T_{ss} - 2T_{us} + T_{uu})]C^2 \right.$$

$$\left. + (\alpha_n^{(s)} + \beta_n^{(s)})\{-3i\mathcal{H}_{ujr}(D-F)^2 - 2i\mathcal{H}_{sjr}(D^2 + 3F^2) + 2i\mathcal{H}_{ss}(D^2 - 3F^2) \right.$$

$$\left. + 2i\mathcal{H}_{us}(D^2 - 6DF + 3F^2) - 3[4R_{ss}F^2 - 4R_{us}F(D-F) + R_{uu}(D-F)^2]\} \right). \tag{C39}$$

$$\langle \Sigma^0|\mathcal{O}^{(0)}_{\mu_0\cdots\mu_n}|\Lambda^0\rangle = 0. \tag{C40}$$

5. Isoscalar helicity matrix elements

$$\langle p|\tilde{\mathcal{O}}^{(0)}_{\mu_0\cdots\mu_n}|p\rangle = \overline{U}_p v_{\{\mu_0}\dots v_{\mu_{n-1}} S_{\mu_n\}} U_p(\Delta\alpha_n^{(s)} + \Delta\beta_n^{(s)}) \times (1 + \mathcal{W}^{(p)}_{\mathrm{SU(6|3)}}) + \frac{\overline{U}_p v_{\{\mu_0}\dots v_{\mu_{n-1}} S_{\mu_n\}} U_p}{f^2}$$

$$\times \left\{\frac{5i}{9}\left(\Delta\gamma_n^{(s)} - \frac{\Delta\sigma_n^{(s)}}{5}\right)(2\mathcal{H}_{uu}^\Delta + \mathcal{H}_{ujr}^\Delta)C^2 + (\Delta\alpha_n^{(s)} + \Delta\beta_n^{(s)})\left[\frac{i}{3}\mathcal{H}_{ujr}(5D^2 - 6DF + 9F^2)\right.\right.$$

$$\left.\left. - \frac{4i}{3}\mathcal{H}_{uu}D(D - 3F) + R_{uu}(D - 3F)^2\right]\right\}. \tag{C41}$$

$$\langle\Lambda^0|\tilde{\mathcal{O}}^{(0)}_{\mu_0\cdots\mu_n}|\Lambda^0\rangle = \overline{U}_{\Lambda^0} v_{\{\mu_0}\dots v_{\mu_{n-1}} S_{\mu_n\}} U_{\Lambda^0}(\Delta\alpha_n^{(s)} + \Delta\beta_n^{(s)}) \times (1 + \mathcal{W}^{(\Lambda)}_{\mathrm{SU(6|3)}}) + \frac{\overline{U}_{\Lambda^0} v_{\{\mu_0}\dots v_{\mu_{n-1}} S_{\mu_n\}} U_{\Lambda^0}}{f^2}$$

$$\times \left(\frac{5i}{9}\left(\Delta\gamma_n^{(s)} - \frac{\Delta\sigma_n^{(s)}}{5}\right)(\mathcal{H}_{us}^\Delta + \mathcal{H}_{uu}^\Delta + \mathcal{H}_{ujr}^\Delta)C^2 + (\Delta\alpha_n^{(s)} + \Delta\beta_n^{(s)})\left\{\frac{2i}{9}\mathcal{H}_{ujr}(7D^2 - 12DF + 9F^2)\right.\right.$$

$$+ \frac{i}{9}\mathcal{H}_{sjr}(D + 3F)^2 - \frac{2i}{9}\mathcal{H}_{uu}(D^2 - 12DF + 9F^2) - \frac{2i}{9}\mathcal{H}_{us}(5D^2 - 6DF - 9F^2)$$

$$\left.\left. + \frac{1}{9}[R_{ss}(D + 3F)^2 - 4R_{us}(2D - 3F)(D + 3F) + 4R_{uu}(2D - 3F)^2]\right\}\right). \tag{C42}$$

$$\langle\Sigma^+|\tilde{\mathcal{O}}^{(0)}_{\mu_0\cdots\mu_n}|\Sigma^+\rangle = \overline{U}_{\Sigma^+} v_{\{\mu_0}\dots v_{\mu_{n-1}} S_{\mu_n\}} U_{\Sigma^+}(\Delta\alpha_n^{(s)} + \Delta\beta_n^{(s)}) \times (1 + \mathcal{W}^{(\Sigma)}_{\mathrm{SU(6|3)}}) + \frac{\overline{U}_{\Sigma^+} v_{\{\mu_0}\dots v_{\mu_{n-1}} S_{\mu_n\}} U_{\Sigma^+}}{f^2}$$

$$\times \left(\frac{5i}{27}\left(\Delta\gamma_n^{(s)} - \frac{\Delta\sigma_n^{(s)}}{5}\right) \times [\mathcal{H}_{uu}^\Delta + 5\mathcal{H}_{us}^\Delta + 2\mathcal{H}_{sjr}^\Delta + \mathcal{H}_{ujr}^\Delta - 2i(T_{ss} - 2T_{us} + T_{uu})]C^2\right.$$

$$+ (\Delta\alpha_n^{(s)} + \Delta\beta_n^{(s)})\left\{\frac{2i}{3}\mathcal{H}_{ujr}(D^2 + 3F^2) + i\mathcal{H}_{sjr}(D - F)^2 - \frac{2i}{3}\mathcal{H}_{uu}(D^2 - 3F^2)\right.$$

$$\left.\left. - \frac{2i}{3}\mathcal{H}_{us}(D^2 - 6DF + 3F^2) + [R_{ss}(D - F)^2 - 4R_{us}F(D - F) + 4R_{uu}F^2]\right\}\right). \tag{C43}$$

$$\langle\Xi^-|\tilde{\mathcal{O}}^{(0)}_{\mu_0\cdots\mu_n}|\Xi^-\rangle = \overline{U}_{\Xi^-} v_{\{\mu_0}\dots v_{\mu_{n-1}} S_{\mu_n\}} U_{\Xi^-}(\Delta\alpha_n^{(s)} + \Delta\beta_n^{(s)}) \times (1 + \mathcal{W}^{(\Xi)}_{\mathrm{SU(6|3)}}) + \frac{\overline{U}_{\Xi^-} v_{\{\mu_0}\dots v_{\mu_{n-1}} S_{\mu_n\}} U_{\Xi^-}}{f^2}$$

$$\times \left(\frac{5i}{27}\left(\Delta\gamma_n^{(s)} - \frac{\Delta\sigma_n^{(s)}}{5}\right) \times [2\mathcal{H}_{ujr}^\Delta + \mathcal{H}_{sjr}^\Delta + \mathcal{H}_{ss}^\Delta + 5\mathcal{H}_{us}^\Delta - 2i(T_{ss} - 2T_{us} + T_{uu})]C^2\right.$$

$$+ (\Delta\alpha_n^{(s)} + \Delta\beta_n^{(s)})\left\{i\mathcal{H}_{ujr}(D - F)^2 + \frac{2i}{3}\mathcal{H}_{sjr}(D^2 + 3F^2) - \frac{2i}{3}\mathcal{H}_{ss}(D^2 - 3F^2)\right.$$

$$\left.\left. - \frac{2i}{3}\mathcal{H}_{us}(D^2 - 6DF + 3F^2) + [4R_{ss}F^2 - 4R_{us}F(D - F) + R_{uu}(D - F)^2]\right\}\right). \tag{C44}$$

$$\langle\Sigma^0|\tilde{\mathcal{O}}^{(0)}_{\mu_0\cdots\mu_n}|\Lambda^0\rangle = 0. \tag{C45}$$

6. Transversity matrix elements

$$\langle p|\tilde{\mathcal{O}}^T_{\mu_0\cdots\mu_n\alpha}|p\rangle = \frac{\overline{U}_p v_{\{\mu_0}\ldots v_{[\mu_n]}S_{\alpha]}U_p[(5+y_1)\delta\alpha_n + 2(1+2y_1)\delta\beta_n]}{6}\times(1+\mathcal{W}^{(p)}_{\text{SU}(6|3)})$$

$$+\frac{\overline{U}_p v_{\{\mu_0}\ldots v_{[\mu_n]}S_{\alpha]}U_p}{f^2}\left(\frac{5i}{81}\left(\delta\gamma_n - \frac{3\delta\sigma_n}{5}\right)(3\mathcal{H}^\Delta_{uu} + \mathcal{H}^\Delta_{ujr})(5+y_1)C^2\right.$$

$$+\frac{8i}{9}\sqrt{\frac{2}{3}}[\mathcal{K}_{uu}(D+3F)(-1+y_1) - \mathcal{K}_{ujr}(3D - F - 2Fy_1)]C\delta c_n$$

$$+\delta\alpha_n\left\{-\frac{1}{6}(5+y_1)(\mathcal{I}_{ujr} - 2i\mathcal{Q}_{uu}) + \frac{i}{3}\mathcal{H}_{ujr}[3D^2 - 6DF + 5F^2 + (D^2+F^2)y_1]\right.$$

$$\left.-\frac{4i}{3}\mathcal{H}_{uu}D(D-2F-Fy_1) + \frac{1}{6}R_{uu}(D-3F)^2(5+y_1)\right\} + \delta\beta_n\left\{-\frac{1}{3}(1+2y_1)(\mathcal{I}_{ujr} - 2i\mathcal{Q}_{uu})\right.$$

$$\left.\left.+\frac{2i}{3}\mathcal{H}_{ujr}[D^2 + F^2(1+2y_1)] - \frac{4i}{3}\mathcal{H}_{uu}D(D-2F-Fy_1) + \frac{1}{3}R_{uu}(D-3F)^2(1+2y_1)\right\}\right). \qquad \text{(C46)}$$

$$\langle\Lambda^0|\tilde{\mathcal{O}}^T_{\mu_0\cdots\mu_n\alpha}|\Lambda^0\rangle = \frac{\overline{U}_{\Lambda^0} v_{\{\mu_0}\ldots v_{[\mu_n]}S_{\alpha]}U_{\Lambda^0}(1+y_1)}{4}[(1+2\tilde{y})\delta\alpha_n + 2\delta\beta_n]\times(1+\mathcal{W}^{(\Lambda)}_{\text{SU}(6|3)})$$

$$+\frac{\overline{U}_{\Lambda^0} v_{\{\mu_0}\ldots v_{[\mu_n]}S_{\alpha]}U_{\Lambda^0}(1+y_1)}{f^2}\left(\frac{5i}{54}\left(\delta\gamma_n - \frac{3\delta\sigma_n}{5}\right)\times[2\mathcal{H}^\Delta_{uu}(1+\tilde{y}) + \mathcal{H}^\Delta_{us}(1+4\tilde{y})\right.$$

$$+\mathcal{H}^\Delta_{ujr}(1+2\tilde{y})]C^2 + \frac{4i}{9}\sqrt{\frac{2}{3}}\{[-\mathcal{K}_{us}(D-3F) + 2\mathcal{K}_{uu}D](1-2\tilde{y}) - \mathcal{K}_{ujr}(D-3F+4D\tilde{y})\}C\delta c_n$$

$$+\delta\alpha_n\left\{-\frac{1}{4}(\mathcal{I}_{ujr} + 2\mathcal{I}_{sjr}\tilde{y} - 2i\mathcal{Q}_{uu} - 4i\mathcal{Q}_{ss}\tilde{y}) + \frac{i}{36}\mathcal{H}_{ujr}[13D^2 - 18DF + 9F^2\right.$$

$$+ 4(5D^2 - 12DF + 9F^2)\tilde{y}] + \frac{i}{36}\mathcal{H}_{sjr}(D+3F)^2 + \frac{i}{18}\mathcal{H}_{uu}[D^2 + 12DF - 9F^2$$

$$- 6(D-3F)(D-F)\tilde{y}] - \frac{i}{18}\mathcal{H}_{us}[(D-3F)(5D+3F) + 2(5D^2 - 9F^2)\tilde{y}] + \frac{1}{36}[R_{ss}(D+3F)^2$$

$$\left.- 4R_{us}(2D-3F)(D+3F) + 4R_{uu}(2D-3F)^2](1+2\tilde{y})\right\} + \delta\beta_n\left\{-\frac{1}{2}(\mathcal{I}_{ujr} - 2i\mathcal{Q}_{uu})\right.$$

$$+\frac{i}{18}\mathcal{H}_{ujr}[(D-3F)^2 + 8D^2\tilde{y}] + \frac{i}{18}\mathcal{H}_{sjr}(D+3F)^2 - \frac{i}{9}\mathcal{H}_{uu}[3(D-3F)(D-F) - 4D^2\tilde{y}]$$

$$+\frac{i}{9}\mathcal{H}_{us}[D^2 + 9F^2 - 12D(D-F)\tilde{y}] + \frac{1}{18}[R_{ss}(D+3F)^2 - 4R_{us}(2D-3F)(D+3F)$$

$$\left.\left.+ 4R_{uu}(2D-3F)^2]\right\}\right). \qquad \text{(C47)}$$

$$\langle \Sigma^+ | \tilde{\mathcal{O}}^T_{\mu_0 \cdots \mu_n \alpha} | \Sigma^+ \rangle = \frac{\overline{U}_{\Sigma^+} v_{\{\mu_0} \dots v_{[\mu_n\}} S_{\alpha]} U_{\Sigma^+} [(5 + y_2)\delta\alpha_n + 2(1 + 2y_2)\delta\beta_n]}{6} \times (1 + \mathcal{W}^{(\Sigma)}_{\text{SU}(6|3)})$$

$$+ \frac{\overline{U}_{\Sigma^+} v_{\{\mu_0} \dots v_{[\mu_n\}} S_{\alpha]} U_{\Sigma^+}}{f^2} \left(\frac{5i}{81} \left(\delta\gamma_n - \frac{3\delta\sigma_n}{5} \right) [\mathcal{H}^\Delta_{uu}(2 + y_2) + \mathcal{H}^\Delta_{us}(13 + 2y_2) + 4\mathcal{H}^\Delta_{sjr} \right.$$

$$+ \mathcal{H}^\Delta_{ujr}(1 + y_2) - 2i(T_{ss} - 2T_{us} + T_{uu})(2 + y_2)]C^2 - \frac{8i}{9}\sqrt{\frac{2}{3}}\{\mathcal{K}_{ujr}(D + F - 2Fy_2)$$

$$+ 2\mathcal{K}_{sjr}(D - F) + [2\mathcal{K}_{uu}F + \mathcal{K}_{us}(D + F)](1 - y_2) - 2i[S_{ss}(D - F) + 2S_{uu}F$$

$$- S_{us}(D + F)](1 - y_2)\}C\delta c_n + \delta\alpha_n\left\{ -\frac{1}{6}(5I_{ujr} - 10iQ_{uu} + [I_{sjr} - 2iQ_{ss}]y_2) \right.$$

$$+ \frac{i}{6}\mathcal{H}_{ujr}[D^2 - 2DF + 5F^2 + 2(D^2 + F^2)y_2] + \frac{5i}{6}\mathcal{H}_{sjr}(D - F)^2 - \frac{i}{3}\mathcal{H}_{uu}[D^2 - 5F^2$$

$$+ (D - F)(D + F)y_2] - \frac{i}{3}\mathcal{H}_{us}[3D^2 - 8DF + 5F^2 - (D^2 + 4DF - F^2)y_2] + \frac{1}{6}[R_{ss}(D - F)^2$$

$$- 4R_{us}F(D - F) + 4R_{uu}F^2](5 + y_2)\bigg\} + \delta\beta_n\bigg\{ -\frac{1}{3}(I_{ujr} - 2iQ_{uu} + 2[I_{sjr} - 2iQ_{ss}]y_2)$$

$$+ \frac{i}{3}\mathcal{H}_{ujr}[(D + F)^2 + 4F^2 y_2] - \frac{2i}{3}\mathcal{H}_{uu}(D^2 - F^2 - 2F^2 y_2) - \frac{2i}{3}\mathcal{H}_{us}[D^2 - 4DF$$

$$+ F^2 - 2F(D - F)y_2] + \frac{i}{3}\mathcal{H}_{sjr}(D - F)^2 + \frac{1}{3}[R_{ss}(D - F)^2 - 4R_{us}F(D - F)$$

$$+ 4R_{uu}F^2](1 + 2y_2)\bigg\}\bigg). \tag{C48}$$

$$\langle \Xi^- | \tilde{\mathcal{O}}^T_{\mu_0 \cdots \mu_n \alpha} | \Xi^- \rangle = -\frac{\overline{U}_{\Xi^-} v_{\{\mu_0} \dots v_{[\mu_n\}} S_{\alpha]} U_{\Xi^-} [(y_1 + 5y_2)\delta\alpha_n + (4y_1 + 2y_2)\delta\beta_n]}{6} \times (1 + \mathcal{W}^{(\Xi)}_{\text{SU}(6|3)})$$

$$+ \frac{\overline{U}_{\Xi^-} v_{\{\mu_0} \dots v_{[\mu_n\}} S_{\alpha]} U_{\Xi^-}}{f^2} \left\{ \frac{5i}{81} \left(\delta\gamma_n - \frac{3\delta\sigma_n}{5} \right) (\mathcal{H}^\Delta_{sjr}(y_1 + y_2) + 4\mathcal{H}^\Delta_{ujr} y_2 + \mathcal{H}^\Delta_{ss}(y_1 + 2y_2) \right.$$

$$+ \mathcal{H}^\Delta_{us}(2y_1 + 13y_2) - 2i(T_{ss} - 2T_{us} + T_{uu})(y_1 + 2y_2))]C^2 - \frac{8i}{9}\sqrt{\frac{2}{3}}[2\mathcal{K}_{ujr}(D - F)y_2$$

$$- \mathcal{K}_{sjr}(2Fy_1 - (D + F)y_2) - \mathcal{K}_{us}(D + F)(y_1 - y_2) - 2\mathcal{K}_{ss}F(y_1 - y_2) + 2i(S_{uu}(D - F)$$

$$+ 2S_{ss}F - S_{us}(D + F))(y_1 - y_2)]C\delta c_n + \delta\alpha_n\bigg[-\frac{1}{6}([I_{ujr} - 2iQ_{uu}]y_1 + 5[I_{sjr} - 2iQ_{ss}]y_2)$$

$$+ \frac{5i}{6}\mathcal{H}_{ujr}(D - F)^2 y_2 + \frac{i}{6}\mathcal{H}_{sjr}(2(D^2 + F^2)y_1 + (D^2 - 2DF + 5F^2)y_2)$$

$$- \frac{i}{3}\mathcal{H}_{ss}((D - F)(D + F)y_1 + (D^2 - 5F^2)y_2) + \frac{i}{3}\mathcal{H}_{us}((D^2 + 4DF - F^2)y_1 - (3D - 5F)$$

$$\times (D - F)y_2) + \frac{1}{6}(4R_{ss}F^2 - 4R_{us}F(D - F) + R_{uu}(D - F)^2)(y_1 + 5y_2)\bigg]$$

$$+ \delta\beta_n\bigg[-\frac{1}{3}(2[I_{ujr} - 2iQ_{uu}]y_1 + [I_{sjr} - 2iQ_{ss}]y_2) + \frac{i}{3}\mathcal{H}_{ujr}(D - F)^2 y_2$$

$$+ \frac{i}{3}\mathcal{H}_{sjr}(4F^2 y_1 + (D + F)^2 y_2) + \frac{2i}{3}\mathcal{H}_{ss}(2F^2 y_1 - (D^2 - F^2)y_2) + \frac{2i}{3}\mathcal{H}_{us}(2F(D - F)y_1$$

$$- (D^2 - 4DF + F^2)y_2) + \frac{1}{3}(4R_{ss}F^2 - 4R_{us}F(D - F) + R_{uu}(D - F)^2)(2y_1 + y_2)\bigg]\bigg\}. \tag{C49}$$

$$\langle\Sigma^0|\tilde{\mathcal{O}}^T_{\mu_0\cdots\mu_n\alpha}|\Lambda^0\rangle = -\frac{\overline{U}_{\Sigma^0}v_{\{\mu_0}\ldots v_{[\mu_n\}}S_{\alpha]}U_{\Lambda^0}(-1+y_1)}{4\sqrt{3}}(\delta\alpha_n - 2\delta\beta_n)\times\left[1 + \frac{1}{2}(\mathcal{W}^{(\Lambda)}_{SU(6|3)} + \mathcal{W}^{(\Sigma)}_{SU(6|3)})\right]$$

$$+ \frac{\overline{U}_{\Sigma^0}v_{\{\mu_0}\ldots v_{[\mu_n\}}S_{\alpha]}U_{\Lambda^0}(-1+y_1)}{\sqrt{3}f^2}\left(-\frac{5i}{54}\left(\delta\gamma_n - \frac{3\delta\sigma_n}{5}\right)(2\mathcal{H}^\Delta_{uu} + \mathcal{H}^\Delta_{us} + \mathcal{H}^\Delta_{ujr})C^2\right.$$

$$+ \frac{4i}{9}\sqrt{\frac{2}{3}}\{2\mathcal{K}_{us}(2D+3F) - \mathcal{K}_{uu}(D-3F) + 2\mathcal{K}_{ujr}D + \mathcal{K}_{sjr}(D+3F) - i[2S_{uu}(2D-3F)$$

$$+ S_{us}(-5D+3F) + S_{ss}(D+3F)]\}C\delta c_n + \delta\alpha_n\left\{\frac{1}{4}(I_{ujr} - 2iQ_{uu}) - \frac{i}{12}\mathcal{H}_{ujr}(D-3F)(3D-F)\right.$$

$$+ \frac{i}{12}\mathcal{H}_{sjr}(D-F)(D+3F) + \frac{i}{3}\mathcal{H}_{uu}D(D+F) + \frac{i}{3}\mathcal{H}_{us}D(D-F) + \frac{1}{12}[R_{ss}(D-F)(D+3F)$$

$$- 4R_{us}(D^2 - 2DF + 3F^2) - 4R_{uu}F(-2D+3F)]\right\} + \delta\beta_n\left\{-\frac{1}{2}(I_{ujr} - 2iQ_{uu})\right.$$

$$- \frac{i}{6}\mathcal{H}_{ujr}(D-3F)(D+F) - \frac{i}{6}\mathcal{H}_{sjr}(D-F)(D+3F) + \frac{2i}{3}\mathcal{H}_{uu}D(D-F) + \frac{2i}{3}\mathcal{H}_{us}DF$$

$$\left.\left.- \frac{1}{6}[R_{ss}(D-F)(D+3F) - 4R_{us}(D^2 - 2DF + 3F^2) - 4R_{uu}F(-2D+3F)]\right\}\right). \tag{C50}$$

APPENDIX D: RESULTS IN SU(2|2)QχPT

In SU(2|2) quenched χPT, the Lagrangian Eq. (12) receives additional contributions since the theory has no axial anomaly and the singlet meson field remains light. Thus,

$$\mathcal{L}^Q_B = i(\overline{\mathcal{B}}v\cdot\mathcal{D}\mathcal{B}) - i(\overline{\mathcal{T}}^\mu v\cdot\mathcal{D}\mathcal{T}_\mu) + \Delta(\overline{\mathcal{T}}^\mu\mathcal{T}_\mu)$$

$$+ 2\alpha(\overline{\mathcal{B}}S^\mu\mathcal{B}A_\mu) + 2\beta(\overline{\mathcal{B}}S^\mu A_\mu\mathcal{B})$$

$$+ 2\mathcal{H}(\overline{\mathcal{T}}^\nu S^\mu A_\mu\mathcal{T}_\nu) + \sqrt{\frac{3}{2}}C[(\overline{\mathcal{T}}^\nu A_\nu\mathcal{B})$$

$$+ (\overline{\mathcal{B}}A_\nu\mathcal{T}^\nu)] + 2\gamma(\overline{\mathcal{B}}S^\mu\mathcal{B})\text{str}(A_\mu)$$

$$+ 2\gamma'(\overline{\mathcal{T}}^\nu S^\mu\mathcal{T}_\nu)\text{str}(A_\mu), \tag{D1}$$

with two additional couplings γ and γ'. There is no relation between the other couplings in Eq. (D1) and those in (PQ)χPT (though we use the same notation for convenience).

Defining

$$\hat{\tau}_3 = \text{diag}(1, -1, \hat{q}, -\hat{q}), \tag{D2}$$

$$\hat{\tau}_0 = \text{diag}(1, 1, 1, 1), \tag{D3}$$

and

$$\hat{\tau}_T = \text{diag}(1, \hat{y}_1, \hat{y}_2, \hat{y}_3), \tag{D4}$$

the quenched χPT twist-two operators correspond (for the most part) to those given in Eqs. (18)–(20) with the replacement $\tau \to \hat{\tau}$ everywhere. Again, the LECs ($\alpha^{(a)}_n$ etc.) occurring in the quenched theory are different from those in $SU(4|2)$ but with this caution, we use the same notation. For the transversity operators one needs additional operators proportional to $\text{str}(\hat{\tau}^{\xi^+_T})$:

$$[\delta\alpha'_n v_{\{\mu_0}\ldots v_{[\mu_n\}}(\bar{\mathcal{B}}S_{\alpha]}\mathcal{B})$$

$$+ \delta\gamma'_n v_{\{\mu_0}\ldots v_{[\mu_n\}}(\bar{\mathcal{T}}^\nu S_{\alpha]}\mathcal{T}_\nu)$$

$$+ \delta\sigma'_n v_{\{\mu_0}\ldots v_{\mu_{n-2}}(\bar{\mathcal{T}}_{\mu_{n-1}}S_{[\alpha}\bar{\mathcal{T}}_{\mu_n]\}})]\text{str}(\hat{\tau}^{\xi^+_T}). \tag{D5}$$

With these definitions it is then easy to calculate the quenched matrix elements in the isospin limit. The wave-function renormalization is

$$\mathcal{W}_{SU(2|2)} = \frac{i}{f^2}[(g_1 + g_A)(6\gamma - g_1 + 2g_A)\mathcal{H}_{uu}$$

$$+ 2g^2_{\Delta N}\mathcal{H}^\Delta_{uu} + (g_1 + g_A)^2 m^2_0\mathcal{H}_{\eta',uu}]. \tag{D6}$$

The isovector, unpolarized matrix element is

$$\langle N|\mathcal{O}^{(3)}_{\mu_0\cdots\mu_n}|N\rangle = \frac{1}{3}\overline{U}_N v_{\mu_0}\ldots v_{\mu_n} U_N(2\alpha^{(a)}_n - \beta^{(a)}_n)\times[1+(1-\delta_{n0})\mathcal{W}_{\mathrm{SU(2|2)}}] + \frac{1}{3f^2}\overline{U}_N v_{\mu_0}\ldots v_{\mu_n} U_N(1-\delta_{n0})$$

$$\times\left(4ig^2_{\Delta N}\left(\gamma^{(a)}_n - \frac{\sigma^{(a)}_n}{3}\right)\mathcal{H}^{\Delta}_{uu} - i(2\alpha^{(a)}_n - \beta^{(a)}_n)\times[6g_A\gamma\mathcal{H}_{uu} + (g_1+g_a)^2 m^2_0\mathcal{H}_{\eta',uu}]\right.$$

$$\left.+ \alpha^{(a)}_n\left\{\frac{3i}{2}g_1[g_1-2(4\gamma+g_A)]\mathcal{H}_{uu}\right\} + \beta^{(a)}_n\left\{\frac{3i}{2}g_1[g_1+2(2\gamma-g_A)]\mathcal{H}_{uu}\right\}\right), \tag{D7}$$

and the isovector, helicity matrix element is

$$\langle N|\tilde{\mathcal{O}}^{(3)}_{\mu_0\cdots\mu_n}|N\rangle = \frac{1}{3}\overline{U}_N v_{\{\mu_0}\ldots v_{\mu_{n-1}}S_{\mu_n\}}U_N(2\Delta\alpha^{(a)}_n - \Delta\beta^{(a)}_n)(1+\mathcal{W}_{\mathrm{SU(2|2)}}) + \frac{1}{3f^2}\overline{U}_N v_{\{\mu_0}\ldots v_{\mu_{n-1}}S_{\mu_n\}}U_N$$

$$\times\left\{\frac{8i}{3}\sqrt{\frac{2}{3}}(g_1+4g_A)\mathcal{K}_{uu}g_{\Delta N}\Delta c_n + \frac{20}{9}ig^2_{\Delta N}\left(\Delta\gamma^{(a)}_n - \frac{\Delta\sigma^{(a)}_n}{5}\right)\mathcal{H}^{\Delta}_{uu} + \frac{i}{3}(2\Delta\alpha^{(a)}_n - \Delta\beta^{(a)}_n)\right.$$

$$\times[6g_A\gamma\mathcal{H}_{uu} + (g_1+g_A)^2 m^2_0\mathcal{H}_{\eta',uu}] - \frac{i}{2}\Delta\alpha^{(a)}_n g_1[g_1-2(4\gamma+g_A)]\mathcal{H}_{uu}$$

$$\left.- \frac{i}{2}\Delta\beta^{(a)}_n g_1[g_1+2(2\gamma-g_A)]\mathcal{H}_{uu}\right\}. \tag{D8}$$

The isoscalar, unpolarized matrix element is

$$\langle N|\mathcal{O}^{(0)}_{\mu_0\cdots\mu_n}|N\rangle = \overline{U}_N v_{\mu_0}\ldots v_{\mu_n} U_N(\alpha^{(s)}_n + \beta^{(s)}_n)\times[1+(1-\delta_{n0})\mathcal{W}_{\mathrm{SU(2|2)}}] + \frac{\overline{U}_N v_{\mu_0}\ldots v_{\mu_n} U_N(1-\delta_{n0})}{f^2}$$

$$\times\left\{\left(\gamma^{(s)}_n - \frac{\sigma^{(s)}_n}{3}\right)\times[2ig^2_{\Delta N}\mathcal{H}^{\Delta}_{uu}] - i(\alpha^{(s)}_n + \beta^{(a)}_n)(g_1+g_A)[(6\gamma - g_1 + 2g_A)\mathcal{H}_{uu}\right.$$

$$\left.+ (g_1+g_A)m^2_0\mathcal{H}_{\eta',uu}]\right\}. \tag{D9}$$

The isoscalar, helicity matrix element is

$$\langle N|\tilde{\mathcal{O}}^{(0)}_{\mu_0\cdots\mu_n}|N\rangle = \overline{U}_N v_{\{\mu_0}\ldots v_{\mu_{n-1}}S_{\mu_n\}}U_N(\Delta\alpha^{(s)}_n + \Delta\beta^{(s)}_n)\times(1+\mathcal{W}_{\mathrm{SU(2|2)}}) + \frac{\overline{U}_N v_{\{\mu_0}\ldots v_{\mu_{n-1}}S_{\mu_n\}}U_N}{f^2}$$

$$\times\left\{\left(\Delta\gamma^{(s)}_n - \frac{\Delta\sigma^{(s)}_n}{5}\right)\times\left[\frac{10i}{9}g^2_{\Delta N}\mathcal{H}^{\Delta}_{uu}\right] + \frac{i}{3}(\Delta\alpha^{(s)}_n + \Delta\beta^{(a)}_n)(g_1+g_A)[(6\gamma - g_1 + 2g_A)\mathcal{H}_{uu}\right.$$

$$\left.+ (g_1+g_A)m^2_0\mathcal{H}_{\eta',uu}]\right\}. \tag{D10}$$

Finally, the transversity matrix elements are

$$\langle N|\tilde{\mathcal{O}}^T_{\mu_0\cdots\mu_n\alpha}|N\rangle = \frac{\overline{U}_N v_{\{\mu_0}\ldots v_{[\mu_n\}}S_{\alpha]}U_N}{6}[(5+\hat{y}_1)\delta\alpha_n + (2+4\hat{y}_1)\delta\beta_n + 6(1+\hat{y}_1-\hat{y}_2-\hat{y}_3)\delta\alpha'_n](1+\mathcal{W}_{\mathrm{SU(2|2)}})$$

$$+ \frac{\overline{U}_N v_{\{\mu_0}\ldots v_{[\mu_n\}}S_{\alpha]}U_N}{f^2}\left(\frac{i}{27}\mathcal{H}^\Delta_{uu}[(6+2\hat{y}_1-\hat{y}_3-\hat{y}_2)(5\delta\gamma_n-3\delta\sigma_n)+6(1+\hat{y}_1-\hat{y}_3-\hat{y}_2)\right.$$

$$(5\delta\gamma'_n-3\delta\sigma'_n)]g^2_{\Delta N} + \frac{4i}{9}\sqrt{\frac{2}{3}}\mathcal{K}_{uu}[4g_A(1-\hat{y}_1)+g_1(4+2\hat{y}_1-3\hat{y}_2-3\hat{y}_3)]g_{\Delta N}\delta c_n$$

$$+ \delta\alpha_n\left\{(-1-\hat{y}_1+\hat{y}_2+\hat{y}_3)\mathcal{I}_{uu} - \frac{1}{9}m_0^2(5+\hat{y}_1)\mathcal{I}_{\eta',uu} + \frac{i}{12}[-g_1^2(2+\hat{y}_3+\hat{y}_2)\right.$$

$$+ 4g_A(g_A(2+2\hat{y}_1-\hat{y}_3-\hat{y}_2)+(5+\hat{y}_1)\gamma)+2g_1(g_A(3+\hat{y}_1-\hat{y}_3-\hat{y}_2)+2(5+\hat{y}_1)\gamma)]$$

$$\times \mathcal{H}_{uu} + \frac{i}{18}(g_1+g_A)^2m_0^2(5+\hat{y}_1)\mathcal{H}_{\eta',uu}\right\} + \delta\beta_n\left\{(-1-\hat{y}_1+\hat{y}_2+\hat{y}_3)\mathcal{I}_{uu} - \frac{2}{9}m_0^2(1+2\hat{y}_1)\right.$$

$$\times \mathcal{I}_{\eta',uu} + \frac{i}{12}[4g_1(2\gamma+g_A+4\gamma\hat{y}_1)+4g_A(2\gamma+g_A+(4\gamma+g_A)\hat{y}_1)+g_1^2(2\hat{y}_1-3(\hat{y}_2+\hat{y}_3))]$$

$$\times \mathcal{H}_{uu} + \frac{i}{9}(g_1+g_A)^2m_0^2(1+2\hat{y}_1)\mathcal{H}_{\eta',uu}\right\} + \delta\alpha'_n\left\{4(\hat{y}_2+\hat{y}_3)\mathcal{I}_{uu} - \frac{2}{3}m_0^2(1+\hat{y}_1-\hat{y}_2-\hat{y}_3)\right.$$

$$\times \mathcal{I}_{\eta',uu} - \frac{i}{3}(g_1+g_A)[g_1-2(3\gamma+g_A)](1+\hat{y}_1-\hat{y}_2-\hat{y}_3)\mathcal{H}_{uu} + \frac{i}{3}(g_1+g_A)^2$$

$$\left.\left.\times m_0^2(1+\hat{y}_1-\hat{y}_2-\hat{y}_3)\mathcal{H}_{\eta',uu}\right\}\right). \tag{D11}$$

[1] J. C. Collins, D. E. Soper, and G. Sterman, Nucl. Phys. **B261**, 104 (1985).

[2] CTEQ Collaboration, R. Brock *et al.*, Rev. Mod. Phys. **67**, 157 (1995).

[3] Y. L. Dokshitzer, Sov. Phys. JETP **46**, 641 (1977); [Zh. Eksp. Teor. Fiz. **73**, 1216 (1977)]; V. N. Gribov and L. N. Lipatov, Yad. Fiz. **15**, 781 (1972); [Sov. J. Nucl. Phys. **15**, 438 (1972)]; L. N. Lipatov, Sov. J. Nucl. Phys. **20**, 94 (1975); [Yad. Fiz. **20**, 181 (1974)]; G. Altarelli and G. Parisi, Nucl. Phys. **B126**, 298 (1977).

[4] J. Pumplin, D. R. Stump, J. Huston, H. L. Lai, P. Nadolsky, and W. K. Tung, J. High Energy Phys. 07 (2002) 012; A. D. Martin, R. G. Roberts, W. J. Stirling, and R. S. Thorne, Phys. Lett. B **531**, 216 (2002); M. Glück, E. Reya, and A. Vogt, Eur. Phys. J. C **5**, 461 (1998).

[5] J. Blümlein and H. Böttcher, Nucl. Phys. **B636**, 225 (2002); Asymmetry Analysis Collaboration, Y. Goto *et al.*, Phys. Rev. D **62**, 034017 (2000); D. de Florian and R. Sassot, Phys. Rev. D **62**, 094025 (2000); E. Leader, A. V. Sidorov, and D. B. Stamenov, Eur. Phys. J. C **23**, 479 (2002).

[6] New Muon Collaboration, P. Amaudruz *et al.*, Phys. Rev. Lett. **66**, 2712 (1991).

[7] E866/NuSea Collaboration, E. A. Hawker *et al.*, Phys. Rev. Lett. **80**, 3715 (1998).

[8] E866/NuSea Collaboration, J. C. Peng *et al.*, Phys. Rev. D **58**, 092004 (1998).

[9] A. W. Thomas, Phys. Lett. **126B**, 97 (1983).

[10] M. Diehl, Phys. Rep. **388**, 41 (2003).

[11] QCDSF Collaboration, M. Göckeler *et al.*, hep-ph/9711245.

[12] W. Detmold, W. Melnitchouk, and A. W. Thomas, Eur. Phys. J. direct C **3**, 1 (2001).

[13] G. Colangelo, hep-lat/0409111.

[14] O. Bär, hep-lat/0409123.

[15] A. Morel, J. Phys. (France) **48**, 1111 (1987).

[16] S. R. Sharpe, Phys. Rev. D **46**, 3146 (1992).

[17] C. W. Bernard and M. F. L. Golterman, Phys. Rev. D **46**, 853 (1992).

[18] C. W. Bernard and M. F. L. Golterman, Phys. Rev. D **49**, 486 (1994).

[19] S. R. Beane and M. J. Savage, Phys. Rev. D **68**, 114502 (2003).

[20] C. W. Bernard and M. F. L. Golterman, Phys. Rev. D **53**, 476 (1996).

[21] M. F. L. Golterman and K. C. Leung, Phys. Rev. D **56**, 2950 (1997); Phys. Rev. D **57**, 5703 (1998); Phys. Rev. D **58**, 097503 (1998).

[22] C. J. D. Lin, G. Martinelli, E. Pallante, C. T. Sachrajda, and G. Villadoro, Nucl. Phys. **B650**, 301 (2003); Phys. Lett. B **553**, 229 (2003); Phys. Lett. B **581**, 207 (2004).

[23] D. Arndt and C. J. D. Lin, Phys. Rev. D **70**, 014503 (2004).

[24] D. Becirevic and G. Villadoro, Phys. Rev. D **69**, 054010 (2004).

[25] W. Detmold and M. J. Savage, Nucl. Phys. **A743**, 170 (2004).

[26] S. R. Beane, P. F. Bedaque, A. Parreño, and M. J. Savage, Phys. Lett. B **585**, 106 (2004).

[27] S. R. Beane, P. F. Bedaque, A. Parreño, and M. J. Savage, Nucl. Phys. **A747**, 55 (2005).

[28] QCDSF-UKQCD Collaboration, A. Ali Khan *et al.*, Nucl. Phys. **B689**, 175 (2004).

[29] S. R. Beane, Phys. Rev. D **70**, 034507 (2004).

[30] S. R. Beane and M. J. Savage, Phys. Rev. D **70**, 074029 (2004).

[31] D. B. Leinweber, A. W. Thomas, K. Tsushima, and S. V. Wright, Phys. Rev. D **64**, 094502 (2001).

[32] R. D. Young, D. B. Leinweber, and A. W. Thomas, Phys. Rev. D **71**, 014001 (2005).

[33] J. Gasser and H. Leutwyler, Phys. Lett. B **188**, 477 (1987); F. C. Hansen, Nucl. Phys. **B345**, 685 (1990); P. Hasenfratz and H. Leutwyler, Nucl. Phys. **B343**, 241 (1990); H. Leutwyler and A. Smilga, Phys. Rev. D **46**, 5607 (1992);H. Leutwyler, Phys. Lett. B **189**, 197 (1987); L. Giusti, C. Hoelbling, M. Lüscher, and H. Wittig, Comput. Phys. Commun. **153**, 31 (2003); L. Giusti, M. Lüscher, P. Weisz, and H. Wittig, J. High Energy Phys. 11 (2003) 023.

[34] W. Detmold and M. J. Savage, Phys. Lett. B **599**, 32 (2004).

[35] P. F. Bedaque, H. W. Grießhammer, and G. Rupak, hep-lat/0407009.

[36] W. Detmold, W. Melnitchouk, J. W. Negele, D. B. Renner, and A. W. Thomas, Phys. Rev. Lett. **87**, 172001 (2001).

[37] D. Arndt and M. J. Savage, Nucl. Phys. **A697**, 429 (2002).

[38] J. W. Chen and X. Ji, Phys. Lett. B **523**, 107 (2001).

[39] J. W. Chen and X. Ji, Phys. Lett. B **523**, 73 (2001).

[40] J. W. Chen and M. J. Savage, Nucl. Phys. **A707**, 452 (2002).

[41] S. R. Beane and M. J. Savage, Nucl. Phys. **A709**, 319 (2002).

[42] J. W. Chen and M. J. Savage, Phys. Rev. D **65**, 094001 (2002).

[43] W. Detmold, W. Melnitchouk, and A. W. Thomas, Phys. Rev. D **66**, 054501 (2002).

[44] W. Detmold, W. Melnitchouk, and A. W. Thomas, Phys. Rev. D **68**, 034025 (2003).

[45] E. Jenkins and A. V. Manohar, Phys. Lett. B **255**, 558 (1991).

[46] E. Jenkins and A. V. Manohar, University of California San Diego Report No. UCSD-PTH-91-30, 1991 (unpublished).

[47] E. Jenkins and A. V. Manohar, Phys. Lett. B **259**, 353 (1991).

[48] V. Bernard, N. Kaiser, and U. G. Meißner, Z. Phys. C **60**, 111 (1993).

[49] J. N. Labrenz and S. R. Sharpe, Phys. Rev. D **54**, 4595 (1996).

[50] M. J. Savage, Nucl. Phys. **A700**, 359 (2002).

[51] D. Arndt and B. C. Tiburzi, Phys. Rev. D **69**, 014501 (2004); Phys. Rev. D **68**, 114503 (2003); **69**, 059904E (2004).Phys. Rev. D **68**, 094501 (2003).

[52] A. Walker-Loud, Nucl. Phys. **A747**, 476 (2005); B. C. Tiburzi and A. Walker-Loud, Nucl. Phys. **A748**, 513 (2005).

[53] B. C. Tiburzi, Phys. Rev. D **71**, 034501 (2005); hep-lat/0412025.

[54] M. Golterman and E. Pallante, J. High Energy Phys. 08 (2000) 023.

[55] W. Detmold, Phys. Rev. D **71**, 054506 (2005).

[56] G. Colangelo and E. Pallante, Nucl. Phys. **B520**, 433 (1998).

[57] G. Martinelli and C. T. Sachrajda, Phys. Lett. B **190**, 151 (1987).

[58] QCDSF Collaboration, M. Göckeler *et al.*, hep-lat/0409162; A. A. Khan *et al.*, hep-lat/0409161.

[59] LHP Collaboration, D. B. Renner *et al.*, hep-lat/0409130.

[60] LHP Collaboration, D. Dolgov *et al.*, Phys. Rev. D **66**, 034506 (2002).

[61] RBCK Collaboration, S. Ohta and K. Orginos, hep-lat/0411008.

[62] QCDSF Collaboration, M. Göckeler *et al.*, hep-ph/0410187.

[63] QCDSF Collaboration, M. Göckeler *et al.*, Phys. Rev. D **53**, 2317 (1996); Nucl. Phys. B, Proc. Suppl. **53**, 81 (1997).

[64] M. Gürtler *et al.*, hep-lat/0409164.

[65] RBCK Collaboration, S. Sasaki, K. Orginos, S. Ohta, and T. Blum, Phys. Rev. D **68**, 054509 (2003).

[66] I. Wetzorke, K. Jansen, F. Palombi, and A. Shindler, hep-lat/0409142.

[67] S. R. Beane, Nucl. Phys. **B695**, 192 (2004).

[68] G. Colangelo and S. Dürr, Eur. Phys. J. C **33**, 543 (2004).

[69] G. Colangelo and C. Haefeli, Phys. Lett. B **590**, 258 (2004).

[70] LHP Collaboration, P. Hägler *et al.*, Phys. Rev. Lett. **93**, 112001 (2004); Phys. Rev. D **68**, 034505 (2003); QCDSF Collaboration, M. Göckeler *et al.*, Phys. Rev. Lett. **92**, 042002 (2004).

[71] J. W. Chen and X. Ji, Phys. Rev. Lett. **88**, 052003 (2002).

[72] A. V. Belitsky and X. Ji, Phys. Lett. B **538**, 289 (2002).

[73] W. Detmold and C.-J. D. Lin, in preparation.

[74] QCDSF Collaboration, M. Göckeler *et al.*, Phys. Lett. B **545**, 112 (2002).

[75] J. W. Chen and M. J. Savage, Phys. Rev. D **66**, 074509 (2002).